# POLE AND ANGLE BASED ANALYSIS OF RR LINKAGES

**By**

**YASH PARIKH**

**A thesis submitted to the**

**School of Graduate Studies**

**Rutgers, The State University of New Jersey**

**In partial fulfillment of the requirements**

**For the degree of**

**Master of Science**

**Graduate Program in Mechanical and Aerospace Engineering**

**Written under the direction of**

**Dr. Haim Baruh**

**and approved by**

**New Brunswick, New Jersey**

**May, 2020**

## ABSTRACT OF THE THESIS

# Pole and Angle Based Analysis of RR Linkages

**by YASH PARIKH**

**Thesis Director:**

**Dr. Haim Baruh**

An infinite number of planar linkage solutions exist for a prescribed rigid body positions. Given a set of precision points, determining fixed pivot and moving pivot curves, sorting through limitless number of possible solutions to find optimal link parameters that satisfies compactness criteria can be a daunting task. In this work, an algorithm is developed and presented by which user can select an optimal linkage from all the mechanism solutions by using Pole and Angle Based Design Method. The significance of poles for design of linkage and hence a mechanism is also determined. The numerical examples presented in this work for two position, three position and four position analysis of a linkage to develop a moving pivot curve using Pole and Angle Based Method have been presented to support analysis capabilities.

**Keywords**: Pole and Angle Based Design Method, RR Linkage Analysis, Numerical Methods

# Acknowledgements

This work would not have been possible without the guidance and assistance of many people around me. I would like to begin by thanking my advisor, Professor Haim Baruh. Alongside being extremely knowledgeable in his field, he is a very genuine and helpful person. Dr. Baruh's door are always open for any questions or any kind of advice. He had an idea behind this project and spent countless hours helping me to get through it.

Great thanks to department of Mechanical and Aerospace Engineering at Rutgers University, New Brunswick for providing me such a platform. All the groundwork for this project was laid in the Graduate class of Design of Mechanisms.

I would like to thank my parents, Hemantkumar and Manisha Parikh for all their love and support throughout my master's degree. A special thanks to my younger brother, Anuj Parikh for always helping me out in every situations. I would also like to thank my other family members and friends for their overall support. Without them, I don't think that I would have accomplished this. My uncle Ketan Shah who as always supported and loved me and my aunt Sweetu Shah who has strengthened me a lot. Friends Vivek Patel, Yashesh Sakharikar and Priyank Thakker have always kept my spirit up and cheered me for years.

# Dedication

To those who stand between us and harm's way on daily basis, asking for nothing in return. Especially to my parents Hemantkumar Parikh and Manisha Parikh, my brother Anuj Parikh and my whole family.

# Table of Contents

# List of Tables

# List of Figures

# Chapter 1

# Introduction

A mechanism is assembled from gears, cams and linkages though it usually contains specialized components such as springs, breaks and clutches. Amongst all of these, the linkage provides versatile movement in any design. A linkage is collection of interconnected components called links which are interconnected by joints. The design of geometric constraints which guides specific movement of a body is called kinematic synthesis.

Kinematic synthesis of design of linkage is the base for kinematic synthesis of design of mechanisms. In the nineteenth century and prior to 1950's, most mechanism analysis and design was done graphically. The algebraic design of mechanisms originated from Freudenstein [1] who is considered as "Father of Modern Kinematics". The Freudenstein equation gives an analytical approach towards analysis and design of four-bar mechanisms which, along with its variants, are present in a large number of machines used in day to day life. The design of linkages which is determined in the thesis is based on design of a guiding linkage by Hall [2], rigid body guidance by Suh and Radcliffe [3], motion generation by Sandor and Erdman [4], and finite-position synthesis by Roth [5]. It is inspired by ideas introduced by Ludwig Burmester [6] for planar movement and Arthur Schoenflies [7] for spatial movement [8]. The texts by Hartenberg and Denavit [9] and Kimbrell [10] gives a detailed development of graphical linkage synthesis. The use of the opposite-pole quadrilateral to construct the center-point curve can be found in Luck and Modler [11].

There are various methods to design linkages such as Graphical Method, Analytical Method and Pole and Angle Based Method. Graphical solutions for the design of a four-bar linkage to accomplish rigid body guidance for up to five positions are known. The previous methods for two and three position synthesis focuses on selecting free choices and then using graphical construction to determine the consequences. If the solution is not satisfactory, new choices are made, and the process is repeated according to Erdman and Sandor [4], Paul B [12] and McCarthy[13]. The traditional graphical method used for design of four position synthesis involved plotting Burmester center point curves using a tedious procedure based on pole quadrilaterals [13], [2].

The algebraic formulation of linkage design was introduced by Freudenstein and Sandor [14] using a complex vector formulation and is developed in detail in the text by Erdman and Sandor [4] and also in Waldron and Kinzel [15]. The polynomial elimination procedure used to solve the RR and PR design equations was inspired by Innocenti [16] and Liao [17]. Computer implementations of planar linkage synthesis originated is carried out using Kaufman's KINSYN [18], and Waldron and Song's RECSYN [19], Erdman and Gustafson's LINCAGES [20], and Ruth's SphinxPC [21]. Ravani and Roth [22] present an optimization approach to linkage synthesis that allows more that five task positions. The analytical synthesis procedure is usually carried out using algebraic solution method unless graphical methods which is less intuitive than any other methods.

The solution of the constraints imposed on the design variables which force the result to be a four-bar linkage, limit the forces and torques within the linkage, restrict the location of the pivot points, limits the lengths of the links, etc. was found using an iterative technique with the aid of a digital computer by Fox and Willmert [23]. Analytical solvers capable of quickly plotting Burmester curves have been developed. In some cases, this software has been integrated into CAD systems. In many cases, this makes the analytical method better suited to solving four-position synthesis problems than the previous graphical technique. However, the analytical method requires software external to the CAD system.

The Pole and Angle Based synthesis approach considered in this thesis changes the focus from making free choices to calculating constraints. The synthesis carried out here is for various positions of the coupler namely two positions, three positions and four positions using Pole and angle based method. After the constraints are known, the available free choices are wisely selected from among all the possible solutions. In most cases, all the possible solutions can be calculated at once knowing the poles and angle of rotations which are defined in the constraints. This is similar to the graphical method given by Zimmerman [24] which gives all the possible solutions using the graphical methods by constructing poles, instead it is an analytical approach. This synthesis method is much faster than conventional analytical approaches and can be applied to the guidance of a rigid body through up to five positions. Known is the fact that the midnormal of the moving pivots in two positions always passes through the pole and that the lines from the moving pivots through the pole are separated by the rotation angle [2]. The angle from the mid-normal line to the line through either moving pivot is consequently half the rotation angle [9]. Using this fact, the need for iterative graphical construction to evaluate possible solutions is eliminated because Pole and angle based method also has a graphical solution method as given in McCarthy [13]. Free choices can be changed if all the possible solutions are not satisfactory and will lead to another definite set of solutions. This synthesis approach removes the time disadvantages of the conventional analytical method has for four and five position synthesis problems.

The geometric theory presented here can be found in Hartenberg and Denavit [9] as well as in Bottema and Roth [25]. The results on the equation of a triangle are drawn from McCarthy [26], while the complex vector formulation follows Erdman and Sandor [4].

For a two position synthesis problem, the previously published literature by Erdman and Sandor[4] recommends using two of the free choices to select moving pivot locations as the first step. The fixed pivots can be located anywhere along the perpendicular bisector of line joining the two links. For each new choice of moving pivots, the construction of perpendicular bisector must be repeated. It was discovered by Loerch [27] [28] for three precision conditions, with one unprescribed angle fixed and the other used as a parameter, fixed pivots and moving pivots of all possible dyads must lie on respective circular loci. For three position synthesis, using both the available free choices to select a moving pivot location is recommended by Paul B [12]. A synthesis is required to identify the fixed pivot location. If the fixed pivot is not suitable, an iterative process is required to find other solutions, requiring repeated graphical construction. For three position synthesis, some have identified that a moving pivot can be found after the fixed pivot is selected by using two poles and their corresponding half rotation angles [13], [2]. Similarly for four position synthesis, fixed and moving pivot curves are determined [29]. Frequent mention is made of the number of free choices, but no mention is made of the constraints.

Each center point choice then requires additional graphical construction to find the corresponding circle point. Circle and center point pairs were then evaluated for suitability. In all of these synthesis problems, the number of free choices was often referenced, but no definition was given for the constraints.

This thesis takes advantage of the property that two lines through the pole separated by half the rotation angle represent a set of possible fixed and moving pivot point pairs, for a two position synthesis problem. When rotated around the pole, these two lines define all the possible fixed and moving pivot point pairs that will satisfy the two specified positions [24]. This pair of lines can be rotated to a desired orientation, and then desirable fixed and moving pivot points can be selected along the lines. This method of linkage design not only simplifies the design process by eliminating the need for iterative conventional analytical solution as well as iterative graphical solution, but also can be extended to three, four and five position synthesis.

This research focuses on the linkage design of a floating link that can be carried for both graphical and analytical construction of a pair of RR linkages. This floating link reaches various positions and points in a defined sets of corresponding points in a fixed frame. The design and synthesis of linkages is challenging and has not been implemented in practice. The design of linkages in this research is based on synthesis of planar chains by poles and rotation angles. This research also includes the results obtained from variation of rotation angle on location of moving pivots for getting a more optimal link design.

# Chapter 2

# Problem Definition

The problem at hand is to study the *Pole and Angle based Method* for design of RR linkages for any four bar mechanism. The dyads are defined by rotation angle $\phi$, location of fixed pivot $G$ and location of moving pivot $W$. The added quantity for design using pole based method is Pole of Displacement $P$. The design equation for RR chain according to J. McCarthy [13] Pole and Angle based method are given as

$$\mathscr{D}_{1i} : (\mathbf{G} - \mathbf{P}_{1i})[A(\phi_{1i}) - I](\mathbf{W}^1 - \mathbf{P}_{1i}) = 0, i = 2, ..., n \tag{2.1}$$

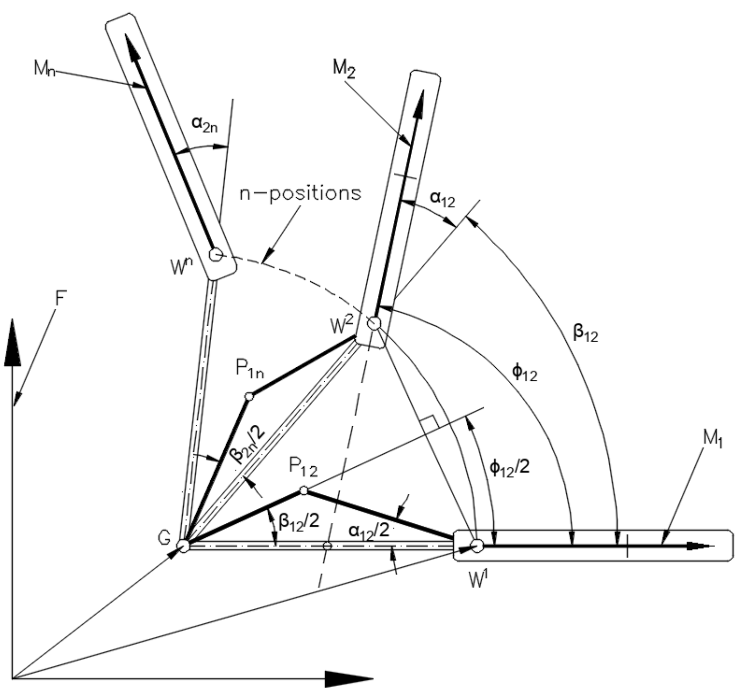


Figure 2.1: Design of RR chain for n-positions of the moving pivot

The pole of displacement gives the location of corresponding link at various instants and forms a curve of link rotation about a fixed pivot along the specified angle of rotation defining the link position within permissible range. The design is compared to conventional linkage design methods as well as graphical methods to understand the location of moving pivot. The design equation for analytical approach for up to four positions according to conventional method described in R. L. Norton [30] is given as

$$W(e^{j\beta_{1k}} - 1) + M(e^{j\alpha_{1k}} - 1) = P_{k1}e^{j\delta_k}, k = 2, 3, 4 \tag{2.2}$$

Here, $P$ denotes the position of linkage at each instant. The angle of rotation $\phi$ is the parameter which is altered to observe the change in location of the linkage. The RR linkage and the parameters of the problem are shown in Figure 2.1.

# Chapter 3

# Methodology

The design of linkages and henceforth mechanisms can be done in many different ways. Graphical and Analytical are the most widely used methods. The position of a moving body at an instant is defined by coordinate transformation and each transformation is associated with an invariant point called the pole of displacement. The relationship between relative positions of points on the moving body and location of pole given by J. McCarthy [13] is used to determine positions of link at various rotation angles.

The approach presented here is based on techniques given in J. McCarthy [13] for motion generation. It is assumed that the designer has identified positions that represent the desired movement of a mechanism. This can be viewed as specifying positions that are to lie in the work space of the linkage. Thus, a discrete representation of the work space is known, but not the design parameters of the linkage. The constraint equations of the chain evaluated at each of the task positions provide design equations that are solved to determine the linkage.

The discussion of pole location and design in this chapter is based on pole and angle based synthesis method given by McCarthy [13]. Similarly, the design of analytical synthesis is based on design analysis given by conventional method discussed in R. L. Norton [30] and Erdman and Sandor [4].

## 3.1 The Pole of Displacement and Angle of Rotation

The displacement between two positions can be achieved by a single rotation about a point called pole of displacement. The pole of displacement is always located in the same ground frame for all the locations of the moving body. The pole of displacement between two positions $M_1 : (\overrightarrow{e}_1, D^1)$ and $M_2 : (\overrightarrow{e}_2, D^2)$ is given as $P_{12}$. The pole of a displacement can be located by using Graphical or Analytical methods.

The points or positions, prescribed for successive locations of the output link in the plane are referred to as precision points or precision positions. The representation of fixed pivot and a moving pivot is a characteristic point representation in any plane which is done by giving x-coordinates and y-coordinates of the point. The ways of representing any point are as follows:

- **Geometric Vectors**: Any point in an $X - Y$ coordinate system can be defined as $X = x\hat{i} + y\hat{j}$.
- **Column Vector Formulation**: The formulation of a point in a single column vector is given as

$$X = \begin{bmatrix} x \\ y \end{bmatrix}$$

- **Complex Variable Notation**: The complex variable representation of a point has a real part and an imaginary part which is $X = x + iy$.

The rotation is described by,

$$\underline{\mathrm{X}} = A\underline{\mathrm{x}} + d$$

where $\underline{\mathrm{x}}$ and $\underline{\mathrm{X}}$ are the initial and final positions in the same reference frame.

The angle of rotation is defined as the angle about which the link rotates at the pole from one precision point to another precision point. The scalar rotation $A[\phi]$ is given as,

$$A[\phi] = \begin{bmatrix} \cos\phi & -\sin\phi \\ \sin\phi & \cos\phi \end{bmatrix}$$

where,

$\phi$ = Angle of Rotation

$d$ = Displacement from one position to another

To find $P_{12}$ graphically, we first consider the point of intersection $C$ of the line through $D_1$ along $\vec{e}_1$ and the line through $D_2$ along $\vec{e}_1$. The angle between these lines about $C$ is called the rotation angle of displacement $\phi_{12}$. Every point in the displaced body moves in a circle about the pole as shown in Figure 3.1.

For each planar rotation there is a unique rotation angle $\phi$, rotation matrix $A$ and translation $d$ associated with which there is a unique pole position $P$. If we consider a case

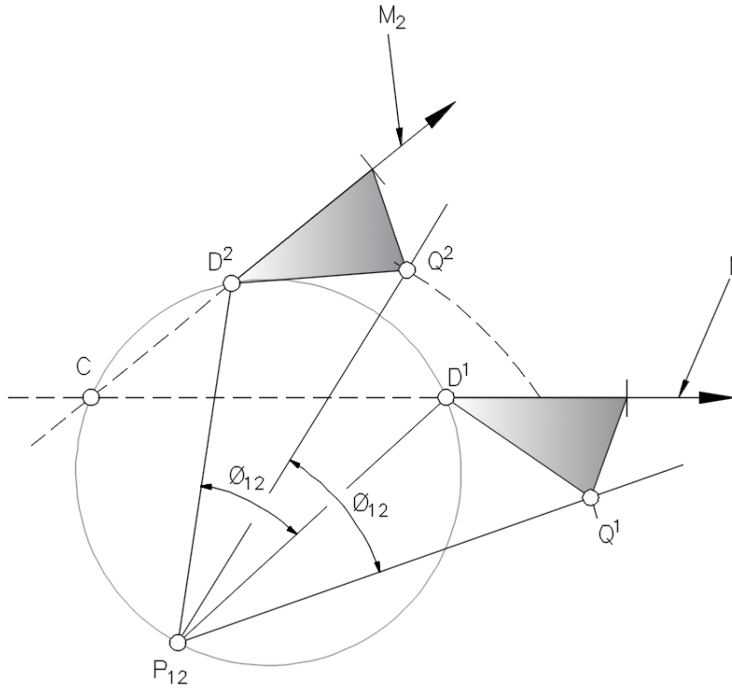


Figure 3.1: A general point $Q_1$ is displaced by a pure rotation about $P_{12}$ by the angle $\phi_{12}$ to the point 2

where we have three positions $M_i$, $i = 1, 2, 3$ for a moving body $M$, the displacements can be considered in pairs to determine poles $P_{12}$, $P_{23}$, $P_{13}$ and the associated rotation angles $\phi_{12}$, $\phi_{23}$, $\phi_{13}$. The displacement given by $T_{13} : (\phi_{13}, P_{13})$ is obtained by a sequence of two successive displacements $T_{12} : (\phi_{12}, P_{12})$ followed by $T_{23} : (\phi_{23}, P_{23})$ as shown in Figure 3.2. Thus,

$$\phi_{13} = \phi_{12} + \phi_{23} \tag{3.1}$$

The three poles $\phi_{13}$, $\phi_{12}$ and $\phi_{23}$ form a triangle known as Pole Triangle as shown in Figure 3.2. The pole $P$ has the coordinates which are unchanged by the planar displacement $[T] = [A(\phi), d]$, that is

$$P = [A(\phi)]P + d \tag{3.2}$$

where,

| | | |
|---|---|---|
| $[T]$ | = | Transformation matrix from one precision point to another |
| $A[\phi]$ | = | Rotation matrix from from one precision point to another |
| $d$ | = | Scalar translation of linkage |

The rotation and translation of linkage are isometric operations i.e. they move on a plane such that distance between point on the body does not change.

The above equation can be solved to determine the coordinates of $P$ as

$$P = [I - A(\phi)]^{-1}d \tag{3.3}$$

where,

$I$ = Identity Matrix

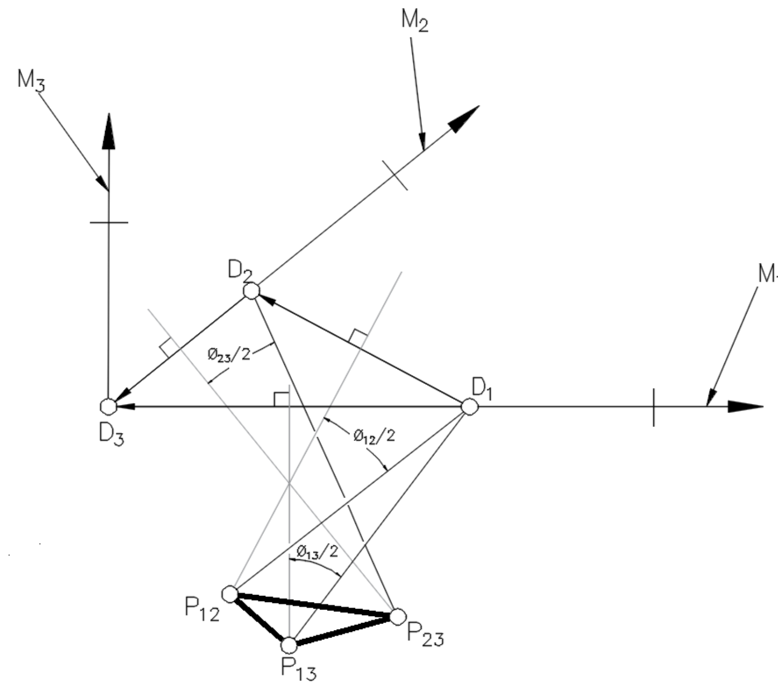


Figure 3.2: The pole triangle associated with three positions $M_1$, $M_2$, and $M_3$

The same equation can also be used to define translation component of the displacement in terms of the coordinates of the pole, that is

$$d = [I - A(\phi)]P \tag{3.4}$$

Thus, a planar displacement $[T] = [A(\phi), d]$ can be defined directly in terms of rotation angle $\phi$ and pole $P$ using Equation 3.2 such that

$$[T(\phi, P)] = [A(\phi), [I - A(\phi)]P] \tag{3.5}$$

### 3.1.1 Pole of Relative Displacement

The pole of the relative displacement from $M_i$ to $M_j$ is found by applying equation 3.3 to the transformation $[T_{ij}] = [A(\phi_{ij}), d_{ij}]$. This can be written in terms of the components of two displacements $[T_i]$ and $[T_j]$ as

$$P_{ij} = [I - A(\phi_{ij})]^{-1}(d_j - A(\phi_{ij})d_i) \tag{3.6}$$

Angle of rotation between $M_1$ to $M_2$ is measured from x-axis of $M_1$ to x-axis of $M_2$. The relative translation vector $d_{12}$ is given in terms of pole $P_{12}$ by

$$d_{12} = [I - A(\phi_{12})]P_{12} \tag{3.7}$$

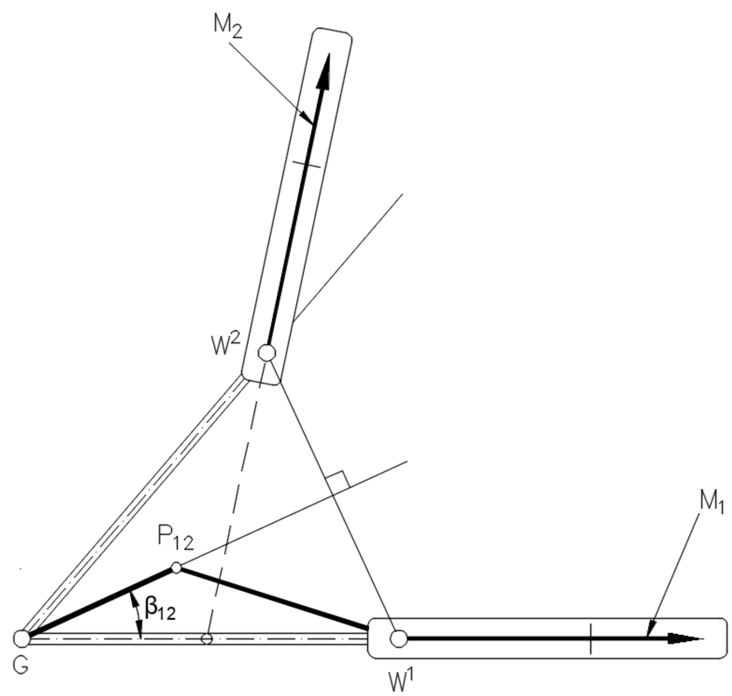


Figure 3.3: The fixed and moving pivots $G$ and $W_1$ of an RR chain and the pole $P_{12}$ from the dyad triangle $\Delta W^1GP_{12}$

## 3.2 Geometry of RR Chain

The displacement of the end-link of RR chain is the result of rotation about the moving pivot $W^1$ followed by a rotation about the fixed pivot $G$ which is equivalent to composition of rotations about the relative poles $P_{12}$ and $P_{23}$, and we find that the *dyad triangle*, $\Delta W^1GP_{12}$ has the same properties as pole triangle. $W^1$ and $W^2$ are corresponding points of the moving pivot in two positions and $G$ is the fixed pivot. The angle $\beta_{12}$ between these lines is the rotation angle of the crank as shown in Figure 3.3. The relative rotation of floating link around $W^2$ is $\alpha_{12}$ between $L^2$ and $\overrightarrow{e}_2$. The relative rotation $\phi_{12}$ of the end-link between positions $M_1$ and $M_2$ is the sum of relative rotations about the fixed and moving pivots,

$$\phi_{12} = \beta_{12} + \alpha_{12} \tag{3.8}$$

which can be found as shown in the Figure 3.4. According to *Burmester's* theory [6] of linkage synthesis, the center point $G$ which is fixed pivot of an RR chain reaches three positions $M_i$, $M_j$, and $M_k$ views the relative poles $P_{ij}$ and $P_{jk}$ in the angle $\beta_{ik}/2$ or $\beta_{ik}/2+\pi$, where $\beta_{ik}$ is the crank rotation angle from position $M_i$ to $M_k$.

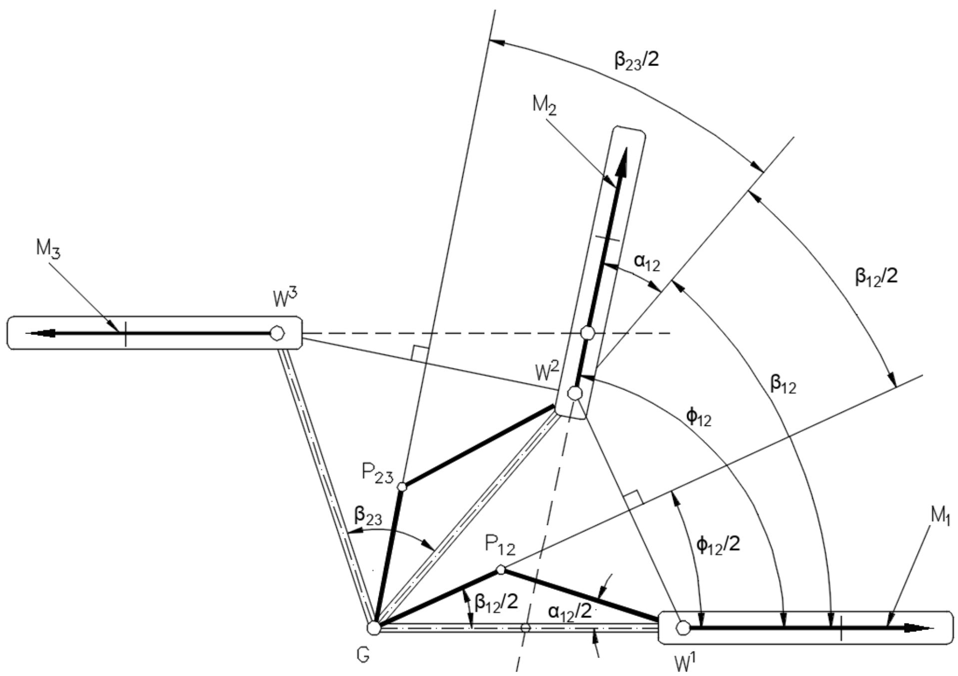


Figure 3.4: The fixed pivot $G$ of an RR chain views the poles $P_{12}$ and $P_{23}$ in the angles $\beta_{12}/2$ and $\beta_{23}/2$ respectively, where $\beta_{13}$ is the crank rotation from position $M_1$ to $M_3$

### 3.2.1 Finite-Position Synthesis of RR Chains

The design of RR chains reaches a specific set of task positions $M_i$. The positions are specified by drawing each reference point $D_i$ and direction vector $\overrightarrow{e}$, where $i = 1, ..., n$, on the background plane $F$.

The fixed pivot $G$ of the RR chain is located in frame $F$ and attached by a link to the moving pivot $W$ in the moving body $M$. The moving pivot defines the corresponding points

$W^i$, $i = 1, ..., n$, in each of the task positions. The points $W^i$ must lie on a circle about $G$, because the crank connecting the $G$ and $W$ has a fixed length. Thus, the goal of the design process is to find points on the rotation circle of moving body that has $n$ corresponding positions on a circle.

### 3.2.2 Polar Synthesis of RR Chain

A revolute, or hinged, joint provides pure rotation about a point. Given two positions of a rigid body, $M_1$ and $M_2$, we can locate a revolute joint such that it moves the body between the two positions. This can be done by locating the hinged joint at the pole of the relative displacement. Let the two positions be specified by the transformations $[T_1] = [A(\phi_1), d_1]$ and $[T_2] = [A(\phi_2), d_2]$. Then, locate the revolute joint $G$ at the relative pole according to equation 3.6 as

$$G = [I - A(\phi_{12})]^{-1}(d_2 - A(\phi_{12})d_1) \tag{3.9}$$

where $\phi_{12} = \phi_2 - \phi_1$ . This joint does not exist if the relative displacement is a pure translation. An RR chain consists of a fixed revolute joint located at a point $G = (x, y)^T$ in $F$ connected by a link to a moving revolute joint located at $w$ in $M$. Let $[T] = [A, d]$ be a displacement that locates $M$. Then the point $W$ in $F$ that coincides with $w$ is given by

$$W = [A]w + d \tag{3.10}$$

where $W = (\lambda, \mu)^T$ must lie on a circle about the fixed pivot $G$, that is,

$$(W - G)(W - G) = (\lambda - x)^2 + (\mu - y)^2 = R^2 \tag{3.11}$$

where $R$ is the length of the link. This geometric constraint characterizes the RR chain. The $n$ positions of the end-link of an RR chain are defined by $[T_i], i = 1, ...., n$ transformations. The coordinates $W^i$ of the moving pivot must satisfy equation 3.11 for each position $M_i$ and $n$ equations are solved simultaneously to get desired output which is given by Burmester as

$$(W^i - W^1)G - \frac{1}{2}(|W^i|^2 - |W^1|^2) = 0, i = 2, ...., n \tag{3.12}$$

which can also be given by,

$$(W^i - W^1)(G - V_{1i}) = 0 \tag{3.13}$$

where $V_{1i} = (W^i + W^1)/2$ is the midpoint of $W^1$ and $W^i$.

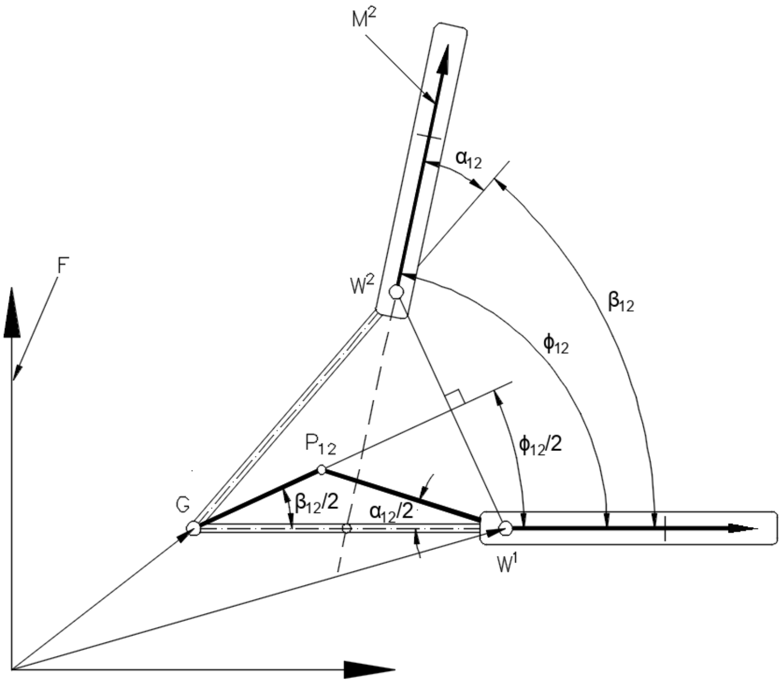


Figure 3.5: The fixed pivot $G$ lies on perpendicular bisector of the segment $W^1W^2$ formed by two positions of the moving pivot

The equation 3.13 shows that $G - V_{1i}$ is perpendicular to $W^i - W^1$ and passes through the midpoint as shown in the figure. This shows that perpendicular bisector of all chords of the circle passes through its center i.e. pole $P_{1i}$ of the relative displacement $[T_{1i}]$ of the end link of RR chain lies on perpendicular bisector of $W^i - W^1$ which gives,

$$(W^i - W^1)(G - P_{1i}) = 0, i = 2, ..., n \tag{3.14}$$

### 3.2.3 Algebraic Design Equations

The design of a RR chain needs identification of a set of task positions $M_i, i = 1, ..., n$, for the end-link of the chain which means that the displacements $[T_i], i = 1, ..., n$, are known, and the angles $\phi_{1i}$ and the relative poles $P_{1i}$ can be determined at the outset. The unknowns are the two coordinates of the fixed pivot $G = (x, y)^T$ and the two coordinates of the moving pivot $W^1 = (\lambda, \mu)^T$ , four in all. The equation 3.14 can be formulated in a way that yields a convenient set of algebraic equations for an RR chain.

$$(W^i - P_{1i}) = [A(\phi_{1i})](W^1 - P_{1i}) \tag{3.15}$$

If we subtract $W^1 - P_{1i}$ from the above equation, we obtain

$$(W^i - W^1) = [A(\phi_{1i}) - I](W^1 - P_{1i}) \tag{3.16}$$

Substituting this into equation 3.14, gives

$$\mathscr{D}_{1i} : (G - P_{1i})[A(\phi_{1i}) - I](W^1 - P_{1i}) = 0, i = 2, ..., n \tag{3.17}$$

which are the design equations for the RR chain. When $n = 4$, we have three design equations in three unknowns. Thus, an RR chain can be designed to reach four arbitrarily specified precision positions.

## 3.3 The Bilinear Structure

The design equations 3.17 are quadratic in the four unknowns $G = (x, y)^T$, $W = (\lambda, \mu)^T$ namely $G_x$, $G_y$, $W_x$ and $W_y$. However, they have the important property that they are linear when considered separately in the unknowns $x, y$, $\lambda$ and $\mu$. This structure provides a convenient strategy for the solution of two to four position problem.

In design of two, three and four precision positions the bi-linear structure provides alternative solutions that we describe as "select the fixed pivot" or "select the moving pivot". These solution strategies correspond to the two ways the design equations can be used to design RR chains. Let the coordinates of the relative pole be $P_{1i} = (p_i, q_i)^T$. Using equation 3.17, we obtain

$$\begin{Bmatrix} x - p_i \\ y - q_i \end{Bmatrix}^T \begin{bmatrix} \cos\phi_{1i} - 1 & -\sin\phi_{1i} \\ \sin\phi_{1i} & \cos\phi_{1i} - 1 \end{bmatrix} \begin{Bmatrix} \lambda - p_i \\ \mu - q_i \end{Bmatrix} = 0, i = 2, ..., n \tag{3.18}$$

If we select the fixed pivot $G$ then the coordinates $x, y$ are known, and we can collect the coefficients of $\lambda$ and $\mu$ to obtain the design equations.

$$A_i(x, y)\lambda + B_i(x, y)\mu = C_i(x, y), i = 2, ..., n \tag{3.19}$$

where,

$$A_i(x, y) = (\cos\phi_{1i} - 1)(x - p_i) + \sin\phi_{1i}(y - q_i),$$
$$B_i(x, y) = -\sin\phi_{1i}(x - p_i) + (\cos\phi_{1i} - 1)(y - q_i),$$
$$C_i(x, y) = (\cos\phi_{1i} - 1)(p_i(x - p_i) + q_i(y - q_i)) + \sin\phi_{1i}(p_i y - q_i x)$$

The coordinates of the moving pivot $(\lambda, \mu)$ are obtained by solving the above set of linear equations. Similarly, if we select the moving pivot $W^1$ then $\lambda, \mu$ are known and we can collect the coefficients of $x$ and $y$ to obtain

$$A'_i(\lambda, \mu)x + B'_i(\lambda, \mu)y = C'_i(\lambda, \mu), i = 2, ..., n \tag{3.20}$$

where,

$$A'_i(\lambda, \mu) = (\cos\phi_{1i} - 1)(\lambda - p_i) + \sin\phi_{1i}(\mu - q_i),$$
$$B'_i(\lambda, \mu) = -\sin\phi_{1i}(\lambda - p_i) + (\cos\phi_{1i} - 1)(\mu - q_i),$$
$$C'_i(\lambda, \mu) = (\cos\phi_{1i} - 1)(p_i(\lambda - p_i) + q_i(\mu - q_i)) + \sin\phi_{1i}(p_i\mu - q_i\lambda).$$

Thus, the fixed pivot coordinates $x, y$ are obtained by solving a set of linear equations, as well.

The equations of the dyad triangle provide a set of design equations that include the crank rotation angles $\beta_{1i}$. These equations provide a way to select a crank angle in the design process. For a set of task positions $M_i = 1, ..., n$, we have the $(n-1)$ dyad triangle equations as discussed in J. McCarthy[13],

$$(1 - e^{i\phi_{1i}})P_{1i} = (1 - e^{i\beta_{1i}})G + e^{i\beta_{1i}}(1 - e^{i\alpha_{1i}})W^1, i = 2, ..., n \tag{3.21}$$

which are linear in the unknown complex vectors $G = x + iy$ and $W^1 = \lambda + i\mu$. If the crank angles $\beta_{1i}$ are specified, then the rotation angles $\alpha_{1i} = \phi_{1i} - \beta_{1i}$ can be calculated.

### 3.3.1 Two Precision Synthesis

If two positions $M_1$ and $M_2$ of the end-link of linkage are specified, then the displacements $[T_1] = [A(\phi_1), d_1]$ and $[T_2] = [A(\phi_2), d_2]$ are given. The relative rotation angle $\phi_{12}$ and the pole $P_{12}$ can be determined. Because $n$=2, there is s single design equation

$$(G - P_{12})[A(\phi_{12}) - I](W^1 - P_{12}) = 0 \tag{3.22}$$

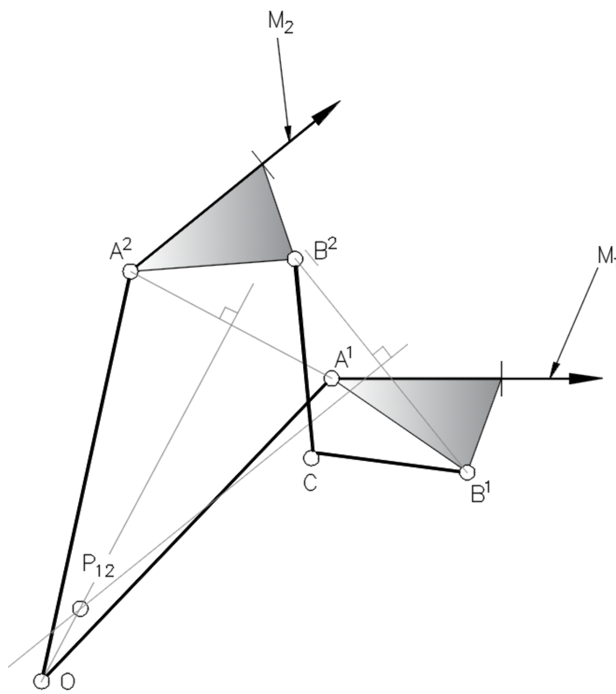


Figure 3.6: Two-Position synthesis of a 4R chain obtained by constructing two different RR open chains and connecting their end-links

To design the RR chain either the fixed or moving pivot can be selected and still have a free parameter.

### Selection of Fixed Pivot for Two Positions

Choose values for the coordinates of the fixed pivot $G = (x, y)^T$, then equation 3.19 yields the equation

$$A_2(x, y)\lambda + B_2(x, y)\mu = C_2(x, y), \tag{3.23}$$

for the coordinates $W^1 = (\lambda, \mu)^T$ of the moving pivot. This equation relates $\lambda$ and $\mu$. One of them is a free choice and the other can be computed.

### Selection of Moving Pivot for Two Positions

The bilinearity of the design equations allows to select values for the coordinates $W^1 = (\lambda, \mu)^T$ of the moving pivot and use equation 3.20 to define

$$A_2'(\lambda, \mu) + B_2'(\lambda, \mu) = C_2'(\lambda, \mu), \tag{3.24}$$

This equation is perpendicular bisector of the line segment $W^1W^2$. Any point on this line can be used as the center point $G$.

## 3.3.2 Three Precision Synthesis

For three specified positions of the floating link, there are three displacements $[T_i] = [A(\phi_i), d_i], i = 1, 2, 3$. Compute the relative angles $\phi_{12}$, $\phi_{13}$ and the poles $P_{12}$, $P_{13}$ in order to obtain the pair of design equations

$$(G - P_{1i})[A(\phi_{1i}) - I](W^1 - P_{1i}) = 0, i = 2, 3 \tag{3.25}$$

These equations yield a unique solution for either fixed pivot $G$ or the moving pivot $W^1$ for an arbitrary choice of another.

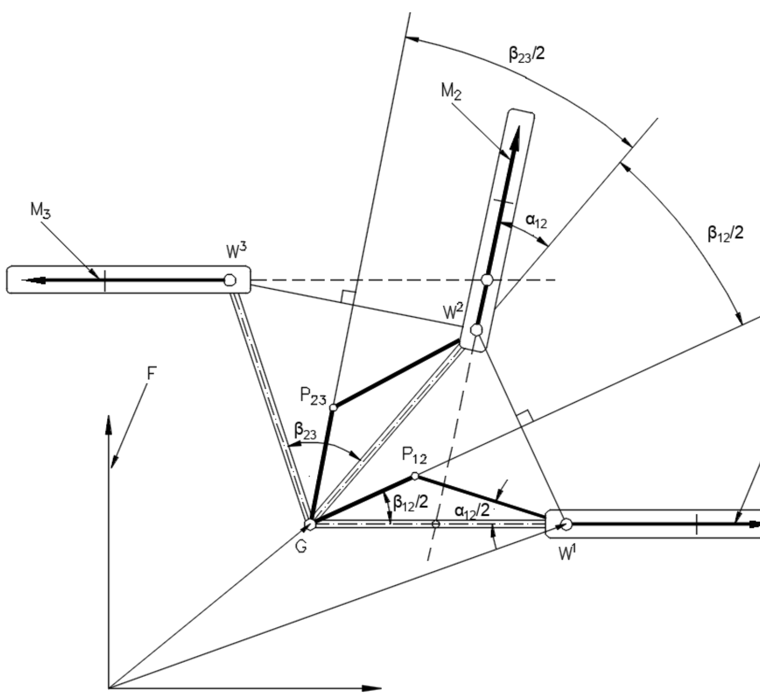


Figure 3.7: The fixed pivot $G$ is the intersection of the two bisectors $V_{12}$ and $V_{23}$

### Selection of Fixed Pivot for Three Positions

Choose values for the coordinates of the fixed pivot $G = (x, y)^T$, then assemble the two design equations 3.19 into a matrix equation

$$\begin{bmatrix} A_1(x,y) & B_1(x,y) \\ A_2(x,y) & B_2(x,y) \end{bmatrix} \begin{Bmatrix} \lambda \\ \mu \end{Bmatrix} = \begin{Bmatrix} C_1(x,y) \\ C_2(x,y) \end{Bmatrix} \tag{3.26}$$

these equations are solved simultaneously to obtain a unique value of moving pivot $W^1$.

### Selection of Moving Pivot for Three Positions

The coordinates of $W^1 = (\lambda, \mu)^T$ are specified and formed into equations 3.20 in matrix to obtain

$$\begin{bmatrix} A_1'(\lambda,\mu) & B_1'(\lambda,\mu) \\ A_2(\lambda,\mu) & B_2(\lambda,\mu) \end{bmatrix} \begin{Bmatrix} x \\ y \end{Bmatrix} = \begin{Bmatrix} C_1'(\lambda,\mu) \\ C_2'(\lambda,\mu) \end{Bmatrix} \tag{3.27}$$

These equations define the two perpendicular bisectors $\mathscr{D}_{12}$ and $\mathscr{D}_{13}$ that intersect at the point $G$.

## 3.3.3 Four Precision Synthesis

For four specified positions of the floating link, $[W_i], i = 1, 2, 3, 4$ should lie on a circle which would not be satisfied by any arbitrary point. There is a cubic curve of moving pivots called the circle-point curve that have four positions on a circle. The center of all these circles form the center-point curve.

If $[M_i], i = 1, 2, 3, 4$ are the four specified positions then relative displacements $[T_{1i}] = [A(\phi_{1i}), d_{1i}]$, the matrix form of the design equations is given as

$$\begin{bmatrix} A_2(x,y) & B_2(x,y) \\ A_3(x,y) & B_3(x,y) \\ A_4(x,y) & B_4(x,y) \end{bmatrix} \begin{Bmatrix} \lambda \\ \mu \end{Bmatrix} = \begin{Bmatrix} C_2(x,y) \\ C_3(x,y) \\ C_4(x,y) \end{Bmatrix} \tag{3.28}$$

gives a solution for the moving pivot $W^1$ only if these equations are linearly dependent.

For these equations to have a solution, the fixed pivot $G$ must be selected so the 3x3

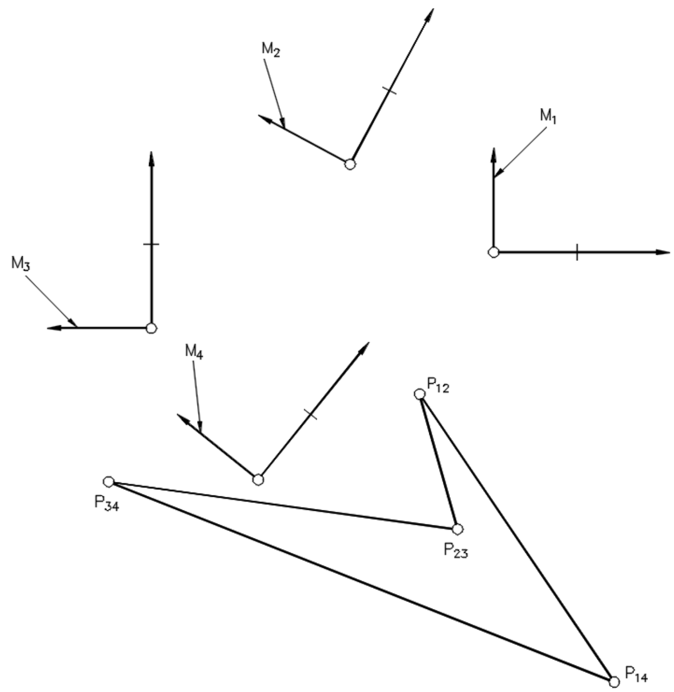


Figure 3.8: The opposite-pole quadrilateral obtained from four planar positions

augmented coefficient matrix $[M] = [A_i, B_i, C_i]$ is of rank two. This means that the determinant $|M|$ equals zero, which yields a cubic polynomial

$$\begin{aligned}\mathscr{R}(x,y) : |M| =& a_{30}y^3 + (a_{21}x^2 + a_{20})y^2 + (a_{12}x^2 + a_{11}x + a_{10})y \\ &+ a_{03}x^3 + a_{02}x^2 + a_{01}x + a_{00} = 0\end{aligned} \tag{3.29}$$

This polynomial defines a cubic curve in a fixed frame, and any point on this curve may be chosen as the center point $G$ for the RR chain, called center-point curve. The coefficients in equation 3.29 are obtained by noting that each of the elements of $[M]$ are linear in the components of $G = (x, y)^T$. Using the column vectors $a_i$,$b_i$ and $c_i$ in the above equation, we have

$$\det[M] = |a_1x + b_1y + c_1, a_2x + b_2y + c_2, a_3x + b_3y + c_3| = 0 \tag{3.30}$$

The above equation can be expanded because of linearity to define coefficients of center-point curve as

$$
\begin{aligned}
a_{30} &= |b_1 b_2 b_3|,\\
a_{21} &= |a_1 b_2 b_3| + |b_1 a_2 b_3| + |b_1 b_2 a_3|,\\
a_{20} &= |b_1 b_2 c_3| + |b_1 c_2 b_3| + |c_1 b_2 b_3|,\\
a_{12} &= |a_1 a_2 b_3| + |a_1 b_2 a_3| + |b_1 a_2 a_3|,\\
a_{11} &= |a_1 b_2 c_3| + |a_1 c_2 b_3| + |b_1 a_2 c_3| + |c_1 a_2 b_3| + |c_1 b_2 a_3|,\\
a_{10} &= |b_1 c_2 c_3| + |c_1 b_2 c_3| + |c_1 c_2 b_3|,\\
a_{03} &= |a_1 a_2 a_3|,\\
a_{02} &= |a_1 a_2 c_3| + |a_1 c_2 a_3| + |c_1 a_2 a_3|,\\
a_{01} &= |a_1 c_2 c_3| + |c_1 a_2 c_3| + |c_1 c_2 a_3|,\\
a_{00} &= |c_1 c_2 c_3|
\end{aligned}
\tag{3.31}
$$

Next we discuss, the *center point theorem* which provides a geometric condition that characterizes center points for four precision positions. For four positions, there are six relative displacement poles $P_{ij}, i < j = 1, 2, 3, 4$, and the center-point theorem requires that a fixed pivot $G$ views the pole pairs $P_{ij}P_{ik}$ and $P_{mj}P_{mk}$ in the angle $\beta_{jk}/2$ or $\beta_{jk}/2 + \pi$. Burmester combined the six relative poles into the three complementary pairs $P_{12}P_{34}$, $P_{13}P_{24}$, and $P_{14}P_{23}$ such that each pair has the numbers 1 through 4 in its indices. He then introduced that opposite pole quadrilateral that has any two of these complementary pairs as its diagonals which ensures that the opposite sides of the opposite pole quadrilateral have the form needed to apply the center-point theorem.

Burmester's Theorem[6] is given as, *"The center point $G$ of an RR chain can reach four specified positions in the plane views opposite sides of an opposite pole quadrilateral obtained from the relative poles of the given positions in angles that are equal, or differ by $\pi$".* This theorem describes a method to derive the center point curve in terms of the coordinates of relative displacement poles. If the opposite pole quadrilateral is formed with vertices $P_{12}P_{23}P_{34}P_{14}$ and the fixed pivot $G$ views $P_{23}P_{12}$ in the angle $\kappa$ and $P_{34}P_{14}$ in $\kappa$ or $\kappa + \pi$. The coordinate direction $\vec{k}$ which is perpendicular to plane, allows us to compute $\sin\,\kappa$ using the vector cross product

$$\vec{k}(P_{12} - G) \times (P_{23} - G) = \sin\kappa |P_{12} - G||P_{23} - G| \tag{3.32}$$

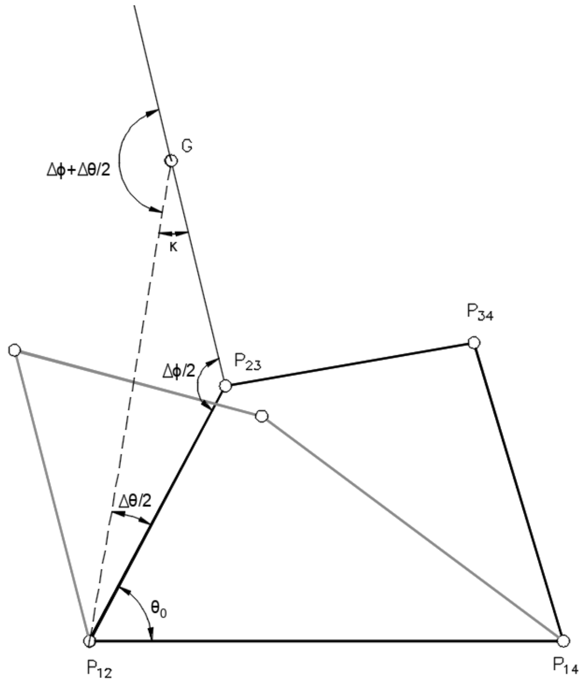


Figure 3.9: The opposite-pole quadrilateral obtained from four planar positions

The value of $\kappa$ is determined by substituting $P_{12} = (p_2, q_2)^T$, $P_{23} = (a_1, b_1)^T$ as

$$\tan\kappa = \frac{(b_1 - q_2)x + (a_1 - p_2)y + p_2 b_1 - q_2 a_1}{x^2 + y^2 - (p_2 + a_1)x - (q_2 + b_1)y + p_2 a_1 + q_2 b_1} = \frac{L_{12}}{C_{12}} \tag{3.33}$$

Similarly for poles $P_{14} = (p_4, q_4)^T$ and $P_{34} = (a_2, b_2)^T$,

$$\tan\kappa = \frac{(b_2 - q_4)x + (a_2 - p_4)y + p_4 b_2 - q_4 a_2}{x^2 + y^2 - (p_4 + a_2)x - (q_4 + b_2)y + p_4 a_2 + q_4 b_2} = \frac{L_{34}}{C_{34}} \tag{3.34}$$

The center point equation given by 3.33 and 3.34 to obtain center point curve is,

$$\mathscr{R}(x, y) : L_{12}C_{34} - L_{34}C_{12} = 0 \tag{3.35}$$

which in cubic terms is,

$$a_{30}y^3 + a_{21}y^2x + a_{12}yx^2 + a_{03}x^3 = ((b_1 - q_2 - b_2 + q_4)x + (a_1 - p_2 - a_2 + p_4)y)(x^2 + y^2) \tag{3.36}$$

The comparison of two, three and four position Pole and angle based Synthesis of RR linkages depending on number of constraints, free choices and solutions is as shown in the Table 3.1.

| No. of Positions | No. of Variables | No. of Prescribed Variables | Constraints | Free Choices | No. of Solutions |
|---|---|---|---|---|---|
| 2 | 6 | 3 | 1 | 3 | $\infty$ |
| 3 | 9 | 6 | 2 | 2 | $\infty$ |
| 4 | 12 | 9 | 3 | 1 | $\infty$ |

Table 3.1: Number of Variables, Constraints and Free Choices Using Poles And Rotation Angles

## 3.4 Analytical Synthesis

Any linkage of a mechanism can be synthesized by closed-form methods for up to five precision points for motion generation with coupler output positions. Analytical synthesis methods are used for solution of any multi-positional synthesis problem by solving simultaneous equations according to Norton[30]. Motion generation technique is the control of a line in the plane such that it assumes some sequential set of prescribe positions. Here the orientation of link containing the line is important. This is accomplished when a point on the coupler traces the desired output path and the linage also controls the angular orientation of coupler link containing the output line of interest. The analytical technique here is used to compare the results obtained by pole based methods. The nomenclature used in this section is similar to nomenclature used in previous chapters.

### 3.4.1 Two Positions Synthesis

This section gives design of a linkage which will move a line on its coupler link such that point $P_i, i = 1, 2$ will be first at $P_1$ and later at $P_2$ and will rotate through an angle $\alpha_2$ between those precision points. The location of the crank is given by positions $A_i, i = 1, 2$. The location of fixed pivot is described by point $G$. The linkage length is given as $W$. Two desired positions are defined in the plane with respect to an arbitrary chosen coordinate system using the position vectors $R_1$ and $R_2$ as shown in the Figure 3.10. The change in angle $\alpha_2$ of the vector $Z_i$ is the rotation required of the coupler link. The position vector $P_{21}$ defines the displacement of the output motion of point $P$ and is defined as:

$$\overrightarrow{P}_{21} = \overrightarrow{R}_2 - \overrightarrow{R}_1 \tag{3.37}$$

The solution is carried out using vector loop equation around the loop which includes both positions $P_1$ and $P_2$.

$$W_2 + Z_2 - P_{21} - Z_1 - W_1 = 0 \tag{3.38}$$

By substituting the complex number equivalents for the vectors, we get

$$we^{j(\theta+\beta_2)} + ze^{j(\phi+\alpha_2)} - p_{21}e^{j\delta_2} - ze^{j\gamma} - we^{j\theta} = 0 \tag{3.39}$$

The terms are simplified and rearranged as,

$$we^{j\theta}(e^{j\beta_2} - 1) + ze^{j\phi}(e^{j\alpha_2} - 1) = p_{21}e^{j\delta_2} \tag{3.40}$$

where,

| | | |
|---|---|---|
| $z$ | = | Link length of Coupler |
| $w$ | = | Link length of Crank |
| $\beta_2$ | = | Rotation angle of Crank between first precision point to second |
| $\alpha_2$ | = | Rotation angle of Coupler between first precision point to second |
| $\theta$ | = | Crank inclination of first position vector with respect to X-axis |
| $\phi$ | = | Coupler inclination of first position vector with respect to X-axis |
| $\delta_2$ | = | Angle between desired output positions |

The lengths of vectors $W_1$ and $W_2$ are of the same magnitude $w$ because they represent the same link in two different positions. This is similar to vectors $M_1$ and $M_2$ in Pole and Angle Based Analysis. Equation 3.40 is a vector equation which is further converted into two scalar equations and can be solved for two unknowns. The equations can be written as, Real Part:

$$\begin{aligned}&[w\cos\theta](\cos\beta_2 - 1) - [w\sin\theta](\sin\beta_2)\\ &\qquad + [z\cos\phi](\cos\alpha_2 - 1) - [z\sin\phi]\sin\alpha_2 = p_{21}\cos\delta_2\end{aligned} \tag{3.41a}$$

Imaginary Part:

$$\begin{aligned}&[w\sin\theta](\cos\beta_2 - 1) - [w\cos\theta](\sin\beta_2)\\ &\qquad + [z\sin\phi](\cos\alpha_2 - 1) - [z\cos\phi]\sin\alpha_2 = p_{21}\sin\delta_2\end{aligned} \tag{3.41b}$$

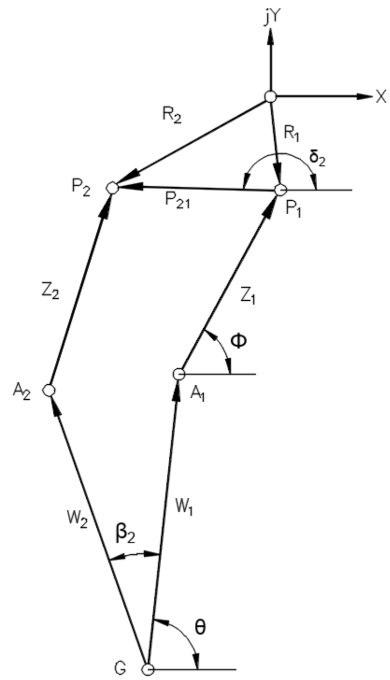


Figure 3.10: A schematic of dyad triangle used for two position vector loop equation

The above two equations have eight variables: $w, \theta, \beta_2, z, \phi, \alpha_2, p_{21}, \delta_2$, and they can be used for solving two unknowns. Out of all the unknowns above, three of the unknowns are defined in the problem statement namely $\alpha_2, p_{21}, \delta_2$. Now, from the remaining five unknowns, $w, \theta, \beta_2, z, \phi$ any three can be considered as free choices and other two can be calculated. Either the angles $\theta, \beta_2, \phi$ are assumed as free choices or we can assume $w, \beta_2, z$. As stated by Norton[30], the commonly used and better approach to design is by selecting $w, \beta_2, z$ as free choices and computing vector $W_1$. Now, $x$ and $y$ components of vectors $M_1$ and $Z_1$ are given as

$$Z_{1_x} = z\cos\phi \qquad\qquad W_{1_x} = w\cos\theta$$

$$Z_{1_y} = z\sin\phi \qquad\qquad W_{1_y} = w\sin\theta$$

Substituting in equation 3.41,

$$W_{1_x}(\cos\beta_2 - 1) - W_{1_y}(\sin\beta_2) + Z_{1_x}(\cos\alpha_2 - 1) - Z_{1_y}\sin\alpha_2 = p_{21}\cos\delta_2$$

$$W_{1_y}(\cos\beta_2 - 1) + W_{1_x}(\sin\beta_2) + Z_{1_y}(\cos\alpha_2 - 1) + Z_{1_x}\sin\alpha_2 = p_{21}\sin\delta_2 \tag{3.42a}$$

The values of $Z_{1_x}$ and $Z_{1_y}$ are known with link length $z$ and rotation angle $\phi$ assumed as free choices. This expression can be further simplified into

$$A = \cos\beta_2 - 1 \qquad B = \sin\beta_2 \qquad C = \cos\alpha_2 - 1$$
$$D = \sin\alpha_2 \qquad E = p_{21}\cos\delta_2 \qquad F = p_{21}\sin\delta_2 \tag{3.43}$$

where,

$$A, B, C, D, E, F \quad = \quad \text{Constants} \tag{3.44}$$

substituting,

$$\begin{aligned} AW_{1_x} - BW_{1_y} + CZ_{1_x} - DZ_{1_y} &= E \\ AW_{1_y} + BW_{1_x} + CZ_{1_y} + Dz_{1_x} &= F \end{aligned} \tag{3.45}$$

The solution is given as,

$$\begin{aligned} W_{1_x} &= \frac{A(-CZ_{1_x} + DZ_{1_y} + E) + B(-CZ_{1_y} - DZ_{1_x} + F)}{-2A} \\ W_{1_y} &= \frac{A(-CZ_{1_y} - DZ_{1_x} + F) + B(CZ_{1_x} - DZ_{1_y} - E)}{-2A} \end{aligned} \tag{3.46}$$

There are infinite solutions to the above problem as any free choices can be selected by the designer. Hence the design of any mechanism is dependent on designers perspective using analytical methods.

### 3.4.2 Three Positions Synthesis

This section gives design of a linkage which will move a line on its coupler link such that point $P_i, i = 1, 2, 3$ will be first at $P_1$ and later at $P_2$ and still later at $P_3$ will rotate through an angle $\alpha_2$ between first two precision points and through an angle of $\alpha_3$ between first and third precision points. The location of the crank is given by positions of moving pivot $A_i, i = 1, 2, 3$. The location of fixed link is described by point $G$. Three desired positions are defined in the plane with respect to an arbitrary chosen coordinate system using the position vectors $R_1$, $R_2$ and $R_3$ as shown in the Figure 3.11. The change in angle $\alpha_2$ and $\alpha_3$ of the vector $Z_i$ is the rotation required of the coupler link. The position vector $\overrightarrow{P}_{21}$ and $\overrightarrow{P}_{31}$ defines the displacement of the output motion of point $D$. Now we will have two vector loop equations to solve for $W_i$ and $Z_i$.

$$W_2 + Z_2 - P_{21} - Z_1 - W_1 = 0$$
$$W_3 + Z_3 - P_{31} - Z_1 - W_1 = 0 \tag{3.47}$$

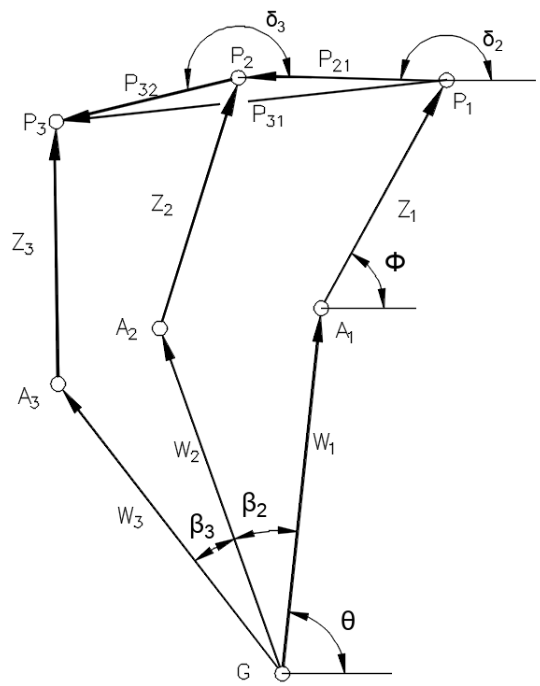


Figure 3.11: A schematic of dyad triangle used for three position vector loop equation

The lengths of vectors $W_1$, $W_2$ and $W_3$ are of the same magnitude $w$ because they represent the same link in three different positions. $M_1$,$M_2$ and $M_3$ whose common magnitude is $m$ are similar to vector $M_i$ in Pole and Angle Based Method. Solving the Equations 3.47 simultaneously by following the same method as we followed in two position synthesis we get four equations, two real parts of the equation and two imaginary parts of the equation as,

Real Part:

$$[w\cos\theta](\cos\beta_2 - 1) - [w\sin\theta](\sin\beta_2)$$
$$+ [z\cos\phi](\cos\alpha_2 - 1) - [z\sin\phi]\sin\alpha_2 = p_{21}\cos\delta_2 \tag{3.48a}$$

$$[w\cos\theta](\cos\beta_3 - 1) - [w\sin\theta](\sin\beta_3)$$
$$+ [z\cos\phi](\cos\alpha_3 - 1) - [z\sin\phi]\sin\alpha_3 = p_{31}\cos\delta_3 \tag{3.48b}$$

Imaginary Part:

$$[w\sin\theta](\cos\beta_2 - 1) + [w\cos\theta](\sin\beta_2) + [z\sin\phi](\cos\alpha_2 - 1) + [z\cos\phi]\sin\alpha_2 = p_{21}\sin\delta_2 \quad (3.48c)$$

$$[w\sin\theta](\cos\beta_3 - 1) + [w\cos\theta](\sin\beta_3) + [z\sin\phi](\cos\alpha_3 - 1) + [z\cos\phi]\sin\alpha_3 = p_{31}\sin\delta_3 \quad (3.48d)$$

The above four equations have twelve variables: $w, \theta, \beta_2, \beta_3, z, \phi, \alpha_2, \alpha_3, p_{21}, p_{31}, \delta_2, \delta_3$, they can be used for solving four unknowns. Out of all the unknowns above, six of the unknowns are defined in the problem statement $\alpha_2$, $\alpha_3$, $p_{21}$, $p_{31}$, $\delta_2$, and $\delta_3$. Now, from the remaining six unknowns, $w, \theta, \beta_2, \beta_3, m, \phi$ any two can be considered as free choices and other two can be calculated. Both the angles $\beta_2, \beta_3$ are assumed as free choices being a simpler approach as it leads to set of linear equations per Norton[30]. Hence it leaves magnitude and orientation of vectors $W$ and $Z$. Now, $x$ and $y$ components of vectors $W$ and $Z$ are given as

$$Z_{1_x} = z\cos\phi \qquad W_{1_x} = w\cos\theta$$

$$Z_{1_y} = z\sin\phi \qquad W_{1_y} = w\sin\theta$$

Substituting in equation 3.48,

$$W_{1_x}(\cos\beta_2 - 1) - W_{1_y}(\sin\beta_2) + Z_{1_x}(\cos\alpha_2 - 1) - Z_{1_y}\sin\alpha_2 = p_{21}\cos\delta_2 \quad (3.49a)$$

$$W_{1_x}(\cos\beta_3 - 1) - W_{1_y}(\sin\beta_3) + Z_{1_x}(\cos\alpha_3 - 1) - Z_{1_y}\sin\alpha_3 = p_{31}\cos\delta_3 \quad (3.49b)$$

$$W_{1_y}(\cos\beta_2 - 1) + W_{1_x}(\sin\beta_2) + Z_{1_y}(\cos\alpha_2 - 1) + Z_{1_x}\sin\alpha_2 = p_{21}\sin\delta_2 \quad (3.49c)$$

$$W_{1_y}(\cos\beta_3 - 1) + W_{1_x}(\sin\beta_3) + Z_{1_y}(\cos\alpha_3 - 1) + Z_{1_x}\sin\alpha_3 = p_{31}\sin\delta_3 \quad (3.49d)$$

This expression can be further simplified into following constants

$$
\begin{aligned}
&A = \cos\beta_2 - 1 && B = \sin\beta_2 && C = \cos\alpha_2 - 1 \\
&D = \sin\alpha_2 && E = p_{21}\cos\delta_2 && F = \cos\beta_3 - 1 \\
&G = \sin\beta_3 && H = \cos\alpha_3 - 1 && I = \sin\alpha_3 \\
&L = p_{31}\cos\delta_3 && M = p_{21}\sin\delta_2 && N = p_{31}\sin\delta_3
\end{aligned} \tag{3.50}
$$

where, $A, B, C, D, E, F, G, H, I, J, K, L, M, N \quad = \quad \text{Constants}$

Substituting,

$$
\begin{aligned}
AW_{1_x} - BW_{1_y} + CZ_{1_x} - DZ_{1_y} &= E \\
FW_{1_x} - GW_{1_y} + HZ_{1_x} - KZ_{1_y} &= L \\
BW_{1_x} + AW_{1_y} + DM_{1_x} + CZ_{1_y} &= M \\
GW_{1_x} + FW_{1_y} + KZ_{1_x} + HZ_{1_y} &= N
\end{aligned} \tag{3.51}
$$

The solution is given by solving the matrix,

$$
\begin{bmatrix} A & -B & C & -D \\ F & -G & H & -K \\ B & A & D & C \\ G & F & K & H \end{bmatrix}
\begin{bmatrix} W_{1_x} \\ W_{1_y} \\ M_{1_x} \\ M_{1_y} \end{bmatrix}
=
\begin{bmatrix} E \\ L \\ M \\ N \end{bmatrix} \tag{3.52}
$$

There are infinite solutions to the above problem as there are free choices $G_x, G_y$. Hence the design of any mechanism is dependent on designers perspective using analytical method for three position synthesis, as well. For a different rotation angle, the calculations are to be carried out again using the same method. While using Pole and Angle based method, all the solutions can be calculated by calculating pole positions.

### 3.4.3 Four Positions Synthesis

The same techniques derived for two and three position synthesis can be extended to four position by adding one more vector loop equation, for an added precision point. The vector loop equations can be formulated in more general form. The angles $\alpha_2$, $\alpha_3$, $\alpha_4$, $\beta_2$, $\beta_3$ and $\beta_4$ will now be designated as $\alpha_k$ and $\beta_k$, $k = 2ton$, where $k$ represents the precision positions and $n = 2, 3, 4$ represents the total number of positions to be solved for. The general vector loop equation now becomes,

$$W_k + Z_k - P_{k1} - Z_1 - W_1 = 0 \qquad k = 2, 3, 4 \tag{3.53}$$

This can be put in a more compact form by substituting vector notations,

$$W = we^{j\theta} \qquad Z = ze^{j\phi} \qquad P_{k1} = p_{k1}e^{j\delta_k} \tag{3.54}$$

then:

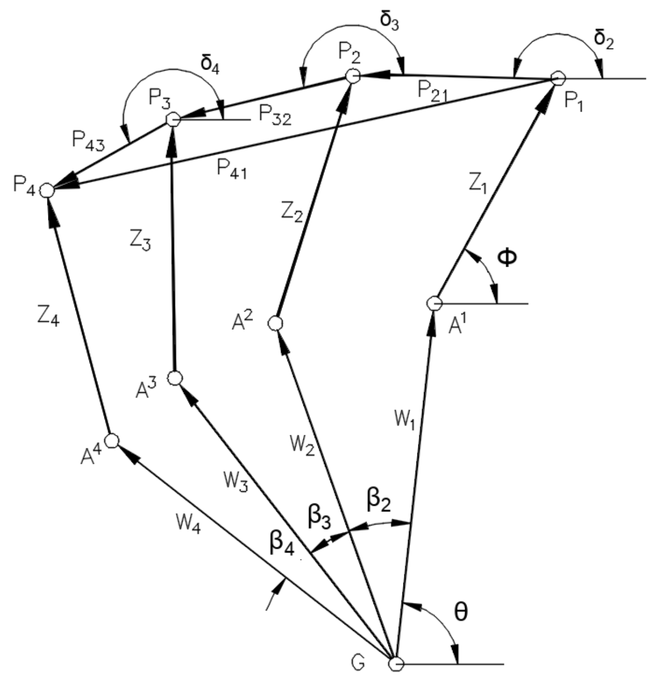


Figure 3.12: A schematic of dyad triangle used for four position vector loop equation

$$W(e^{j\beta_k} - 1) + Z(e^{j\alpha_k} - 1) = P_{k1}e^{j\delta_k} \tag{3.55}$$

Here, $P$ denotes the precision points which is denoted as $D$ in Pole and Angle based approach by McCarthy [13]. Equation 3.55 is called the standard form equation by Erdman and Sandor [4]. The above equation for four position analysis has sixteen variables $w$, $\theta$, $\beta_2$, $\beta_3$, $\beta_4$, $z$, $\phi$, $\alpha_2$, $\alpha_3$, $\alpha_4$, $p_{21}$, $p_{31}$, $p_{41}$, $\delta_2$, $\delta_3$, $\delta_4$ forming six equation. The circle point and center point circles of the three position problem become cubic curves called Burmester curves in four position problem. Here we can only solve the equation for six variables and out of remaining ten variables, nine are already defined in the statement problem. So, there is just one free choice. The defined variables are $\beta_2$, $\beta_3$, $\beta_4$, $p_{21}$, $p_{31}$, $p_{41}$, $\delta_2$, $\delta_3$ and $\delta_4$. If we define the angle $\theta$ as a free choice, the variables which we are going to calculate are $w$, $\alpha_2$, $\alpha_3$, $\alpha_4$, $z$ and $\phi$.

There are infinite solutions to the above problem depending upon the selection of free choices which is according to designer's perspective. The Analytical method does not provide definite solution for all the precision points except for free choices selected for a specified precision point.

The comparison of two, three and four position Analytical synthesis of RR linkages depending on number of constraints, free choices and solutions is as shown in the Table 3.2.

| No. of Positions | No. of Variables | No of Equations | No. of Prescribed Variables | Free Choices | No. of Solutions |
|---|---|---|---|---|---|
| 2 | 8 | 2 | 3 | 3 | $\infty$ |
| 3 | 12 | 4 | 6 | 2 | $\infty$ |
| 4 | 16 | 6 | 9 | 1 | $\infty$ |

Table 3.2: Number of Variables, Constraints and Free Choices Using Analytical Synthesis Method

## 3.5 Graphical Synthesis

The RR chains reaches a specific set of task positions $M_i$ by drawing reference point $D_i$ and direction vector $\overrightarrow{e}^i$, i=1,...,n on the background plane $F$. The fixed pivot $G$ of RR chain is attached by a link to the moving pivot $W$ in moving body $M$. The points $W^i$ must lie on a circle about $G$, because crank connecting $G$ and $W$ has a constant length.

### 3.5.1 Two Precision Positions

For two positions $M_1 : (\overrightarrow{E}_1, D^1)$ and $M_2 : (\overrightarrow{E}_2, D^2)$, a moving pivot $W^1$ has a second position $W^2$ in frame $F$. The fixed pivot $G$ lies on the perpendicular bisector of the line segment $W^1W^2$. Any point on this line can be chosen as the fixed pivot of the chain with

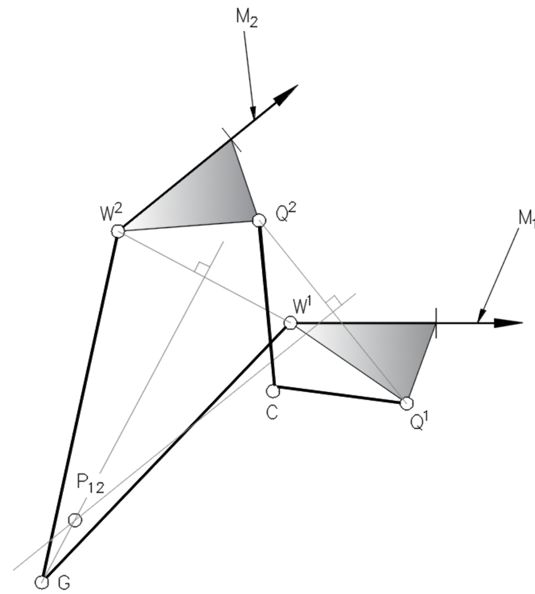


Figure 3.13: The fixed pivot $G$ of an RR chain lies on the perpendicular bisector of the segment $W^1W^2$

$W^1$ as the moving pivot.

For each choice of a moving pivot $W^1$ there is a one dimensional set of fixed pivots $G$. Thus, there is a three dimensional set of RR chains compatible with the two positions. It is most preferable to select fixed pivot $G$ rather than selecting moving pivot. This is done by locating the pole $P_{12}$ and determining the relative rotation $\phi_{12}$ of displacement from $M_1 : (\overrightarrow{E}_1, D^1)$ to $M_2 : (\overrightarrow{E}_2, D^2)$. The line $V = GP_{12}$ must be the perpendicular bisector of the segment $W^1W^2$ for a specific fixed pivot $G$ for all possible moving pivots $W^1$. The angle $\phi_{12}/2$ can be drawn on either side of line V around $P_{12}$ to construct lines $L^1$ and $L^2$. Any point on line $L^1$ can be determined as moving pivot $W^1$. The circle about $P_{12}$ with radius $P_{12}W^1$ intersects $L^2$ on the point $W^2$.

### 3.5.2 Three Precision Positions

For the three positions $M_i : (\overrightarrow{E}_i, D^i)$, i=1,2,3, the moving pivot $W^1$ for $M_1$ moves to the points $W^2$ and $W^3$ in the other two positions. The desired fixed pivot $G$ is the center of the circle through $\Delta W^1W^2W^3$.

The construction is done by first constructing the poles $P_{12}$ and $P_{13}$ and the rotation angles $\phi_{12}$ and $\phi_{13}$. Then selecting a fixed pivot $G$ and joining it to the poles $P_{12}$ and $P_{13}$ by

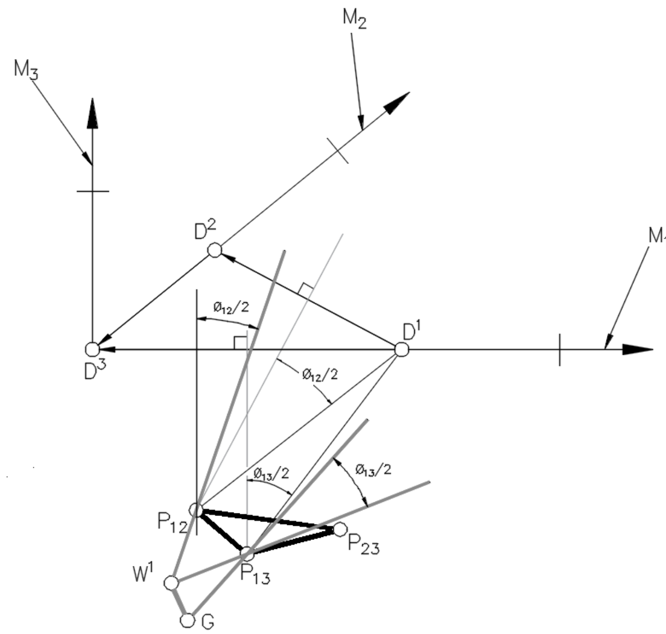


Figure 3.14: The moving pivot $W^1$ determined using selected fixed pivot $G$ and the pole triangle

lines $V_{12}$ and $V_{13}$. Thus, duplicating angle $\phi_{12}/2$ on either side of $V_{12}$ to define lines $L^1$ and $L^2$, and angle $\phi_{13}/2$ on either side of $V_{13}$ to define the lines $M^1$ and $M^2$. The intersection of two lines $L^1$ and $M^1$ defines the moving pivot $W^1$.

### 3.5.3 Four Precision Positions

For four positions of the moving body, $W^i, i = 1, 2, 3, 4$, there are points on the moving body $M$ that have four corresponding points $W^i$ that lie on the circle as described by Burmester's theorem that defines the desired RR chains by constructing opposite-pole quadrilateral. The six relative displacement poles $P_{ij}, i \leq j = 1, 2, 3, 4$ are assembled into three opposite pole pairs i.e. $P_{12}P_{34}$, $P_{13}P_{24}$ and $P_{14}P_{23}$.

The construction is carried out by first constructing the opposite-pole quadrilateral $Q : P_{12}P_{23}P_{34}P_{14}$ using the relative poles of the four task positions. Then selecting an arbitrary angle $\theta$ and rotating the segment $P_{12}P_{23}$ by this angle about $P_{12}$ to obtain $P'_{23}$. Now, we can construct a new location of $P_{34}$ on a circle about $P_{14}$ such that $P'_{34}$ maintains its original distance to $P'_{23}$.

The new configuration $Q'$ of the quadrilateral $Q$. The pole $G$ of the displacement of the

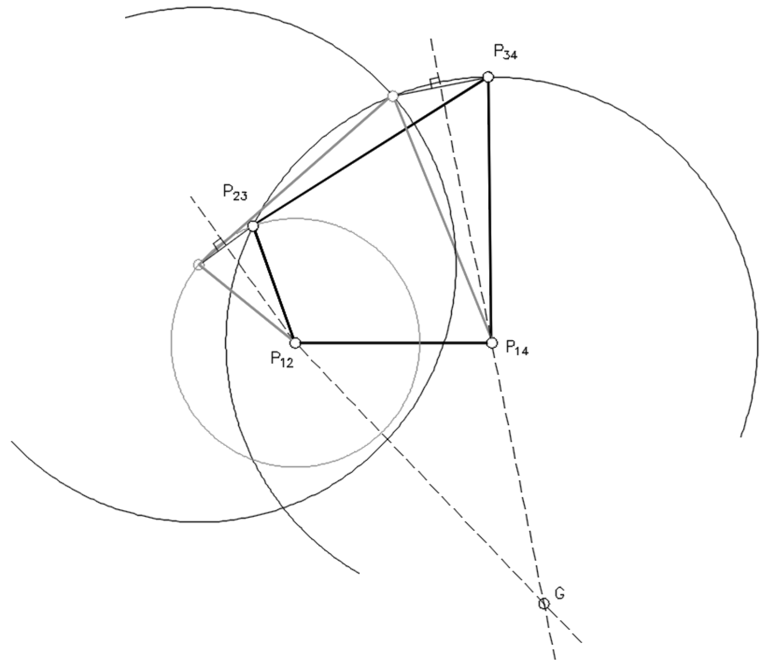


Figure 3.15: A fixed pivot $G$ for four specified positions is constructed using the quadrilateral formed by the poles $P_{12}P_{23}P_{34}P_{14}$

segment $P'_{23}P'_{34}$ relative to its original location $P_{23}P_{34}$ that satisfies Burmester's theorem and is a center point $G$.

The relative poles obtained from all of the configurations of the opposite-pole quadrilateral form a cubic curve known as the center-point curve. Once a center point is obtained by this construction, any three of the four positions can be used to construct the associated moving pivot. The result is an RR chain that reaches the four specified positions.

# Chapter 4

# Design of RR chains

## 4.1 Introduction to Design and Simulation

In the previous chapter, Pole and Angle based design, analytical synthesis and graphical synthesis methods for two, three and four position analysis of RR chains are presented. In all the design methods, there are constraints and free choices depending on the number of prescribed positions. The design basis of RR chain on pole and angle based method as described by J. McCarthy [13], the classical design of RR chain is as described in classical texts such as R.L.Norton [30] which are then compared to the graphical synthesis method and importance of Pole and Angle based method is shown. In this chapter, the design of the location of fixed pivot $G$ and locus of moving pivot $W^i$ of RR chain is presented using all the three methods and the results are compared to show the importance of Pole and Angle based method over the other two methods. The design is carried out using MATLAB and Simulink.

The simulation of position analysis is carried out by considering constraints and free choices of different position synthesis. When the coupler is guided through two precision points, there are three free choices and one constraint for each guiding link. One constraint is added by adding each coupler position which results in reducing a free choice. For the number of positions that our analysis is carried on, constraints and free choices are summarized in the Tables 3.1 & 3.2 in previous chapter.

## 4.2 Selecting Constraints and Free Choices

Selection of constraints basically depends on design requirements of a mechanism and also on designers choice. A comparison of constraint and free choices selection is defined in this chapter by analyzing two different cases. The first case defines the fixed pivot $G$ and rotation angle $\phi$ and carrying out design of moving pivot $W^i$ for two positions, three positions and four positions. The second case defines moving pivot $W^i$ and angle of rotation $\phi$ and designing for fixed pivot $G$. One can select free choices blindly and design a linkage blindly using design approach or one can use guidelines to follow to select free choices and carry out the design. According to Zimmerman [24], defining fixed pivot and angle of rotation and then analyzing moving pivot is better suited for design of mechanisms. This provides optimal length of links required and output positions so as to design a mechanism accordingly which gives maximum coupler output according to application requirements by using minimal input.

A distinct advantage of pole and angle based method is that the fixed and moving pivot options can be seen and selected simultaneously as by the location of poles obtained from the calculations. The synthesis methods require graphical construction to find the fixed pivot after the moving pivot is selected or vice versa. The other key advantage is that no additional construction is required to evaluate new fixed and moving point pairs if the original choice is not suitable. If the design is to be evaluated for more than one desired locations of coupler link of mechanism, then evaluation of other points on the basis of location of pole can be done using pole and angle based method by just defining rotation angle.

## 4.3 Design Algorithm

Figure 4.1 illustrates a diagram of the algorithm developed in this work. Moving pivot curves are generated numerically by using Pole and Angle Based design given in J. McCarthy[13]. This section explains the detailed method followed in linkage design.

The first step, as shown in block A1, of the algorithm is defining the constraints of the given RR linkage. For our case, the predefined variables includes the desired pivot locations for two, three or four position synthesis. The rotation angle $\phi$ is also defined in the problem. Although depending on the positions that synthesis has to be carried out, the constraints change to the number of equations that can be solved to obtain respective free choices.

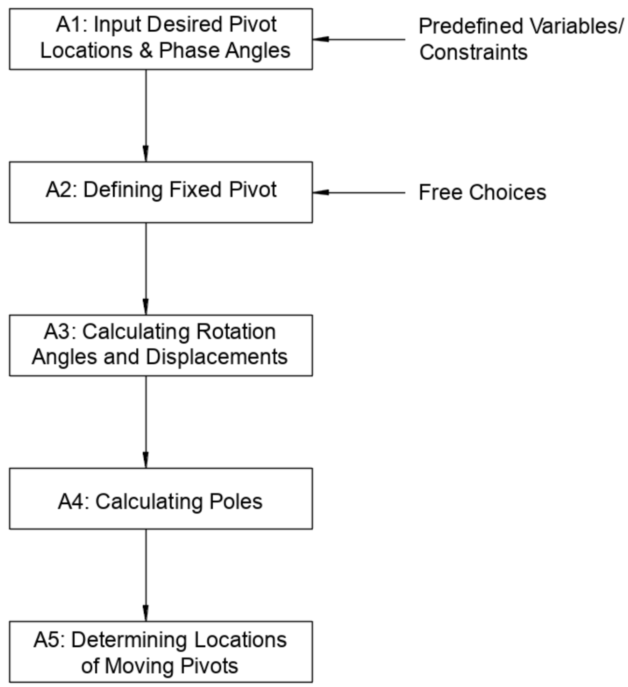


Figure 4.1: Design algorithm of Two, Three and Four Precision Points by Pole & Angle Based Method

The second step, in the algorithm (block A2), defines the free choices of RR linkage. The fixed pivot $G$ is also defined as a free choice. Similar to number of constraints, number of free choices also change depending on various position synthesis according to Pole and Angle based design method.

The third step, given in block A3, involves calculation of the rotation matrix $A[\phi]$ and displacement $d$. The rotation matrices are calculated according to various rotation angles for different positions. And hence displacement are calculated on the basis of rotation matrices between various positions.

The fourth step, given in block A4, involves calculation of pole of displacement from one position to another positions. According to user defined free choices, solutions are carried out computationally. The accuracy of pole position is one of the most important factors of design using this method as it gives various solutions using this pole positions.

The fifth step, as in block A5, involving calculation of the moving pivots $W^i$ for the defined desired positions, phase angles and fixed pivots. The pole positions used to find fixed pivot locations which are obtained from pole positions lie on a circle of rotation of moving pivot. The accuracy of the results obtained from pole and angle based methods compared with results obtained from analytical synthesis i.e. conventional design method and graphical method. Alongside that, the rotation angle are varied to a certain range to see the deviation in location of moving pivot with the same fixed pivot using pole locations, describing importtance of pole locations.

## 4.4 Two Position Design Approach

For two position simulation according to pole and angle based method, unknowns are fixed pivot $G = (G_x, G_y)$ and moving pivot $W^i = (\lambda, \mu)$. The coupler precision points $D_i$ are given as input conditions to the problem with a specified angle of rotation $\phi_{12}$ from first location to second location of coupler motion. The designer can select free choices knowing the circumstances of desired output. Selecting the fixed pivot as free choices leads to infinite solutions of a moving pivot and can lead to undesirable link lengths. Though selecting a fixed pivot as free choice, designer still has to select either $\lambda$ or $\mu$ from the moving pivot locations because two position synthesis results in one algebraic equation which can only be solved for one variable. Now, selection of coordinate of moving pivot constrains the link to a desired range. Hence, both poles and rotation angles here are used as constraints. The rotation from the moving pivots to the fixed pivot position is in the same direction as the rotation angle. The general representation of Pole and Angle Based two position analysis is as illustrated in Figure 4.2.

The designer can quickly see all the possible solutions by rotating the linkage around the pole according to rotation angle required to reach the desired position.

The moving pivot line is shown dashed and fixed pivot line is solid. Additionally, fixed and moving pivot lines usually are shown terminating at the pole, when in fact, these lines extend infinitely in both directions. The general form of the constraint is shown in Figure 4.2 for any two positions $X$ and $Y$ where the rotation angle is not zero.

A number of textbook illustrations of RR linkage for two position synthesis were evaluated using pole based, analytical and graphical methods to verify solutions, one of which is described here.

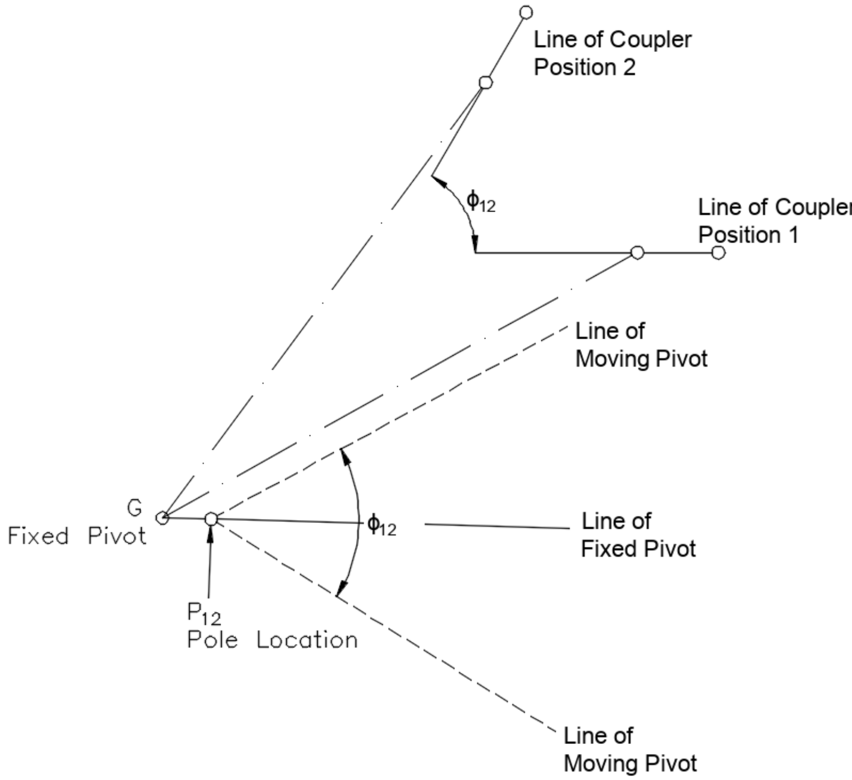


Figure 4.2: Pole and Angle Based Design for Two Position Analysis

The target position points are given as $D_1 = (7, 3)$ and $D_2 = (2, 7)$ and the angle of rotation between them is given by $\phi_{12} = 60°$. The design of RR chain is carried out by selecting free choices and then calculating the moving pivots of the coupler. The fixed pivot $G$ is selected as free choice as an origin of the coordinate system $(0, 0)$. The $x$ co-ordinate of $W$ i.e. $\lambda$ is set to a certain value, for our case it is set to $\lambda = 1$. The moving pivots $W^i, i = 1, 2$ are calculated by first calculating pole position $P_{12}$. Refer to MATLAB code as in Appendix 1. The MATLAB code is formulated on basis of the pole based design approach for two positions discussed in previous chapter. The analysis is also carried out on the basis of variation of the rotation angle $\phi_{12}$ to determine the precision of the moving pivot with respected to selected fixed pivot from the actual desired location.

Analytical solution is also carried out for the same problem according to methods given in R.L. Norton [30] as explained in section previous chapters. Graphical solution to the above problem is also done to calculate the location of moving pivots.

## 4.5 Three Position Design Approach

For three position synthesis, two constraints must be satisfied simultaneously. If we choose to do the synthesis on the moving body in position one, then the constraints are defined by the poles $P_{12}$ and $P_{13}$ and the rotation angles $\phi_{12}$ and $\phi_{13}$. The two constraints are the fixed pivots $D_i$ and rotation angles $\phi_{ij}$ for $i, j = 1, 2, 3, i < j$. The poles are separated by half of the respective rotation angles. The moving pivot lines for first position intersect at point $W_1$ as shown in the figure which is similar for second position $W_2$and third position $W_3$.

The fixed pivot lines intersect at the fixed pivot $G$, as shown in the figure. The moving pivot line for position two from $P_{12}$ and the moving pivot line for position three from $P_{13}$ are taken into consideration but not shown in the Figure 4.3.

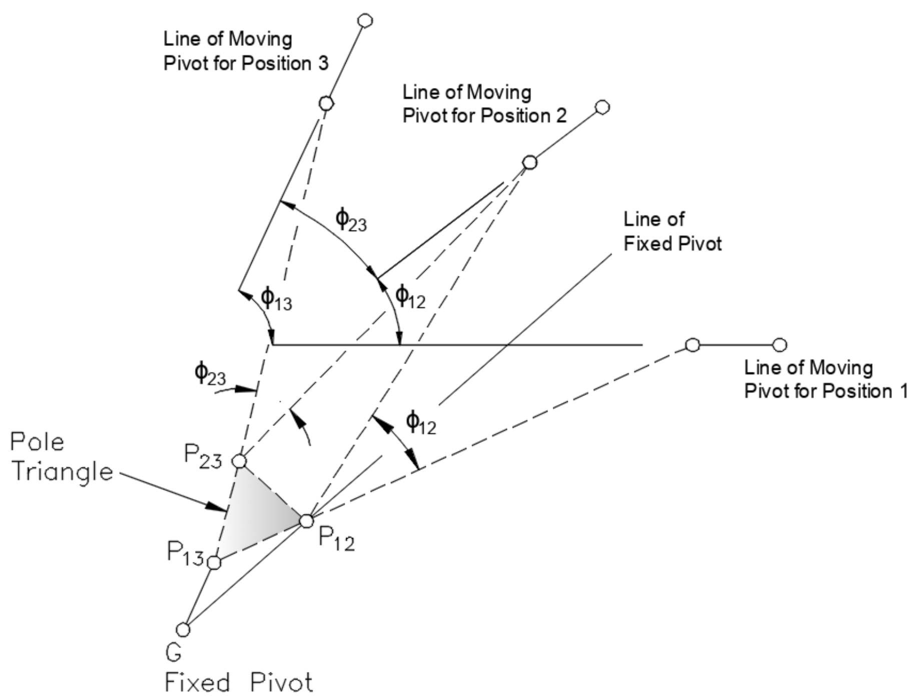


Figure 4.3: Pole and Angle Based Design for Three Position Analysis

All of these pairs of lines can be rotated to any angle in the plane, so that either the fixed or moving pivot can be placed anywhere the designer desires. All of the possible solutions can be seen in a few seconds by changing the fixed pivot in the plane and observing the corresponding location of the moving pivot. The moving pivot could also be moved in the plane and the location of the fixed pivot can be observed. Hence, both the cases of analysis can be verified and compared for selection of free choices.

The free choices are the Cartesian coordinates of location of fixed pivot $G$. The rotation angles $\phi_{12}$ and $\phi_{13}$ are in same direction, therefore the moving pivot lines are in the same direction from pole $P_{12}$ are also in the same direction of those from pole $P_{13}$.

A textbook illustration of three positions is evaluated using pole and angle based method, analytical method and graphical method to demonstrate the location of moving pivots. The coupler target positions are given as $D_1 = (0, 8)$, $D_2 = (7, 4)$ and $D_3 = (1, 6)$. The rotation angle $\phi_{ij}, i, j = 1, 2, 3, i < j$ is given as 30° i.e. $\phi_{12} = 30°$ and $\phi_{13} = 60°$. The rotation matrix $[A(\phi)]$ is determined from the rotation angles along with translation $d_{ij}, i, j = 1, 2, 3, i < j$ from one position to another position.

The poles are calculated using equation 3.6. The fixed pivot is defined as a free choice $G = (0, 0)$. The coefficients of $\lambda$ and $\mu$ are defined using equation 3.19. $\lambda$ and $\mu$ are hence formulated in the matrix form to calculate $W^i, i = 1, 2, 3$. The variation in the rotation angle is also carried out Refer to MATLAB code formulated on the basis of pole based design approach for three positions discussed previous chapter. Refer to Appendix 2.

Analytical solution to the same statement problem is also carried out according to method described in previous section as given by R. L. Norton [30]. The analytical simulation is also carried out using MATLAB to demonstrate the location of moving pivots. A graphical solution is also done to calculate the location of moving pivots.

## 4.6 Four Position Design Approach

For four position synthesis, a third constraint is added. Again, this constraint is the line of the moving pivot $W_4$ and the line of the fixed pivot $G$ passing through the pole $P_{14}$ and separated by half the rotation angle $\phi_{14}$. The pole and corresponding fixed and moving pivot lines for positions one and four are added and shown in Figure 4.4. The four fixed pivot lines can be constrained to intersect at a single point. When this is done, the three corresponding moving pivot lines for position one will not necessarily intersect at a common point. The fixed pivot $G$ point can be moved in the plane until the moving pivot lines do intersect at a single point. The moving pivot lines can then be constrained to have a common intersection point. This identifies one center point, circle point pair.

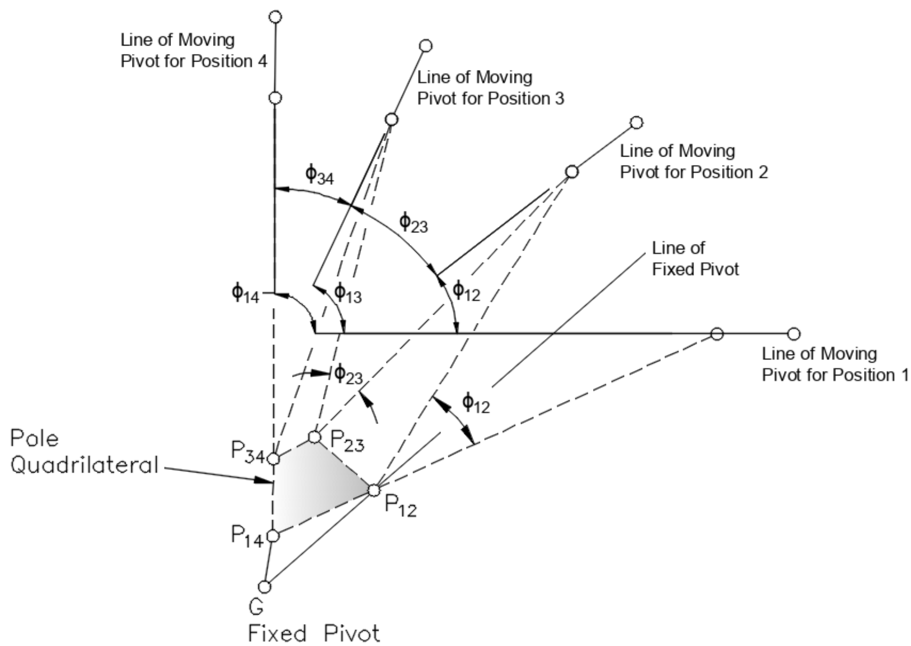


Figure 4.4: Pole and Angle Based Design for Four Position Analysis

Once the three constraints are selected, only one free choice remains. The center point or the circle point can be moved in the plane. However, the motion is constrained to the center and circle point curves. As either point is moved in the plane, the circle and center point curves are traced simultaneously. If the center point curve is continuous, all the circle and center point pairs can be seen by dragging either point along its curve. The free choice is made by selecting a circle-center point pair.

The center points are on the fixed body $G$ and the circle points are on the moving body in the position represented by the common subscript $W^1$, $W^2$, $W^3$ and $W^4$. The pole positions are shown in Figure 4.4 as $P_{12}$, $P_{23}$, $P_{34}$ and $P_{14}$ that are used in the construction of the curves. In summary, any three poles having a common subscript and their corresponding rotation angles defines the constraints. These three constraints define both the circle and center point Burmester's curves simultaneously. As the circle and center point curves are traced, individual pairs of points can be considered. This is a new technique for solving the four position synthesis problem and constructing Burmester's curves graphically, as well. The constraints force the matching points to remain on the Burmester's curves [6]. This method provides infinite resolution for selecting circle-center point pairs along the curves. The circle point curve is specific to the position for which we do the synthesis. For example, the circle point curve for the body in position two is rotated from the circle point curve for the body in position one.

A textbook illustration of four positions of a textbook mechanism were evaluated using pole based methods, analytical methods and graphical methods to compare the locations of moving pivot positions. The target positions for the mechanism are given as $D_1 = (12, 3)$, $D_2 = (7, 7)$, $D_3 = (4, 9)$ and $D_4 = (2, 7)$. The angles of rotation are given as $\phi_{12} = 30°$, $\phi_{13} = 60°$ and $\phi_{14} = 90°$. Similar to two and three position synthesis, the rotation angles were also varied to understand the behavior of the moving pivots $W^1$, $W^2$, $W^3$ and $W^4$ from the desired coupler output. One of the coordinates of fixed pivot $G$ is considered to be a free choice and selected accordingly. The coordinate positions of moving pivots are calculated using MATLAB using an iterative loop in the research. Refer to Appendix 3.

Analytical solution is also carried out for the same problem using method described in previous chapter by R. L. Norton [30]. The same example is also solved using graphical method to check the accuracy of pole and angle based method.

# Chapter 5

# Results

## 5.1 Two Position Method Results

The two position design gives solution according to conventional method, Pole and Angle Based and Graphical method using the design approaches given in previous chapters. The solution and their comparison are provided in the following section. Various textbook problems were evaluated for two position design out of which one of the problem is as follows. Consider an initial positions of coupler as $D_1 = 7i + 3j$ and second position as $D_2 = 2i + 7j$. In the problem, rotation from first position to second position is given as $60°$. In the above problem, the fixed pivot position is considered to be at (0,0) as a free choice. Alongside $\lambda = 1$, i.e., $X$ co-ordinate of moving pivot is also considered as a free choice.

The solution of the above problem by Pole and angle based method is carried out by the method described in previous chapter which is from J. McCarthy [13]. A solution of the same problem using conventional method is carried out according to method followed in previous chapter which follows method defined in Norton [30]. The graphical solution of two position problem which was done using AutoCAD is compared to solution obtained by Analytical as well as Pole and Angle based method carried out in Matlab (described in Appendix A) and variation is observed. The comparison of results obtained from all the three methods is as shown in the following Table 5.1. The values of moving pivots obtained

| | Location of Moving Pivot W1 | Location of Moving Pivot W2 |
|---|---|---|
| Graphical Method | (1.48,1.53) | (2,0.71) |
| Analytical Method | (1.4759,1.5291) | (2,0.7185) |
| Pole and Angle Based Method | (1.4758,1.5291) | (2,0.7185) |

Table 5.1: Comparison of Solutions from Graphical, Analytical and Pole and Angle Based Methods for Two Position Problem

from all the methods in Table 5.1 shows that the results obtained are accurate. As described in previous chapters, from a pole position we can get all the solutions for the angles that we want to reach. Let us assume here that our link rotates following the Grashof's criteria [31], and our crank rotates by an angle of $\phi$. According to the theory, the angle between initial and final location of moving pivot about the pole $P_{12}$ is equal to the phase angle $\phi_{12}$ which rotates from 5° to 60°. Here using the assumed location of fixed pivot, angle of rotation and already calculated Pole location $P_{12}$, we can find the location of all the points that our link reaches using that pole location. Using the following range of variable $\phi_{12}$:

$$\phi_{12} = 5°,\ 10°,\ \ldots,\ 60°$$

As the prescribed phase angle $\phi_{12}$ increases, the moving pivot $W^i$ is observed to rotate from $W^1$ to $W^n$ about the pole $P_{12}$ which is calculated to be as $(1.0359, 0.6699)$.

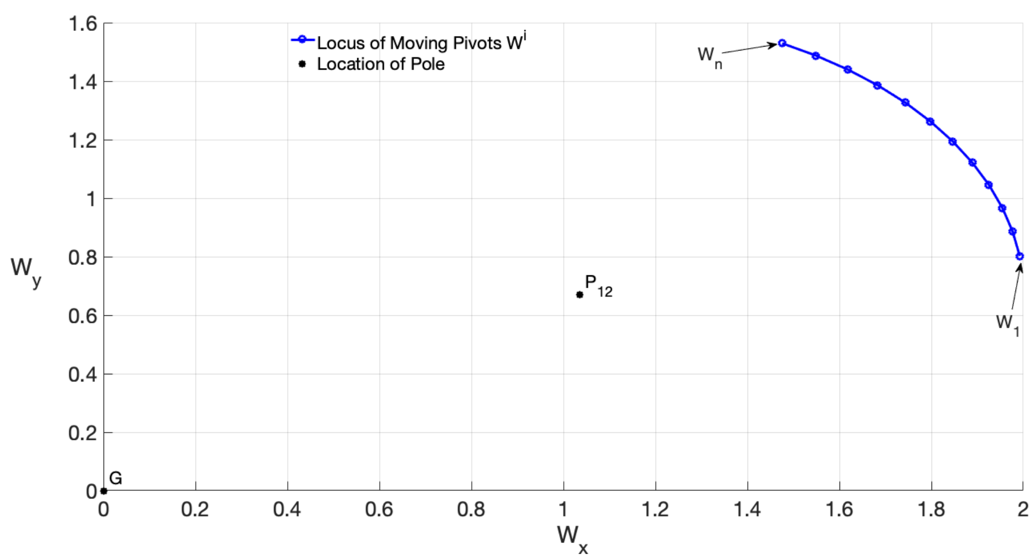


Figure 5.1: Locus of Moving Pivot $W^x$ and $W^y$ over Pole $P_{12}$

The abscissa is in Figure 5.1 represents the $X$ co-ordinate of the moving pivot $W^i$ and ordinate represents the $Y$ co-ordinate of moving pivot $W^i$. The blue link indicates the locus of moving pivots. From the output it is observed that the moving pivot $W^i$ rotates around fixed pivot $G$ with a constant link length where $W^1$ is the initial position of moving pivot at 0° and $W^n$ is the position of moving pivot at 60°.

The abscissa is in Figure 5.2 represents the $X$ co-ordinate of moving pivot $W^i$ and ordinate represents the phase angle $\phi_{12}$. The blue line indicates the locus of moving pivots

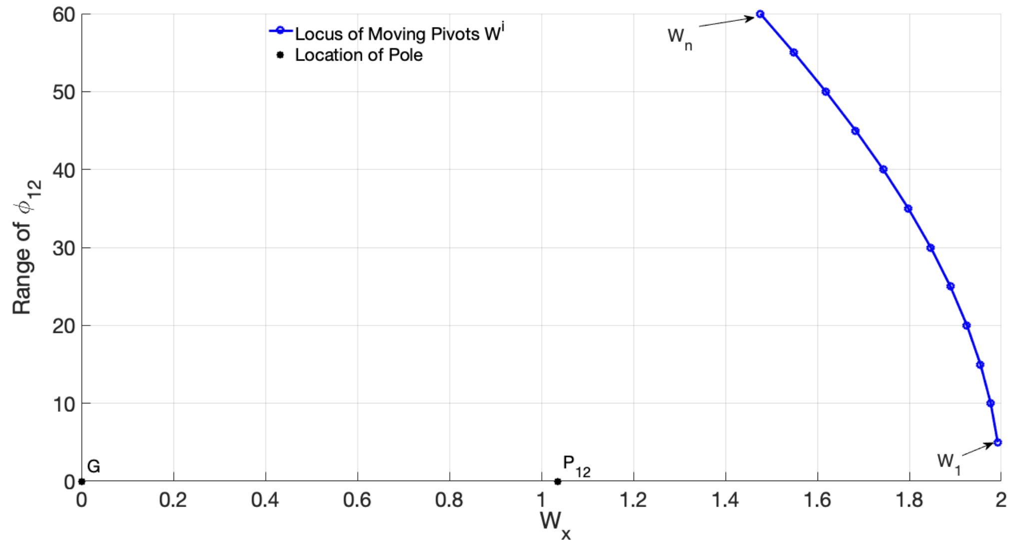


Figure 5.2: Locus of $X$ co-ordinate of Moving Pivot $W^x$ over Pole $P_{12}$

$W^i$.

The abscissa is in Figure 5.3 represents the $Y$ co-ordinate of moving pivot $W^i$ and ordinate represents the phase angle $\phi_{12}$.

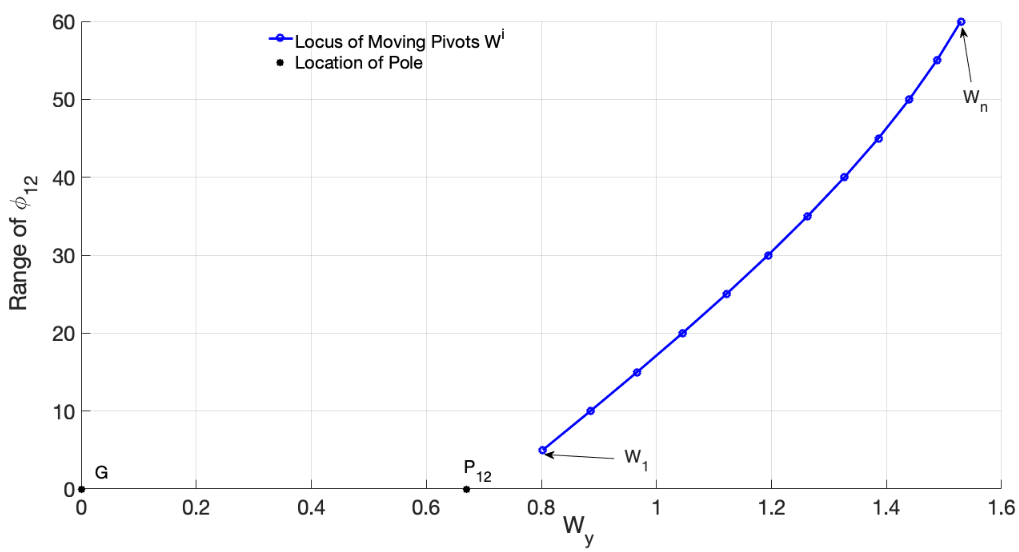


Figure 5.3: Locus of $Y$ co-ordinate of Moving Pivot $W^y$ over Pole $P_{12}$

$X$-axis on the Figure 5.4 represents the $X$ co-ordinates of moving pivot, $Y$-axis represents $Y$ co-ordinate of moving pivot and $Z$-axis represents the increase in phase angle defined in the problem. From the plots it is observed that moving pivot rotates around fixed pivot with a constant link length about the pole $P_{12}$. Using the pole, all the values of moving

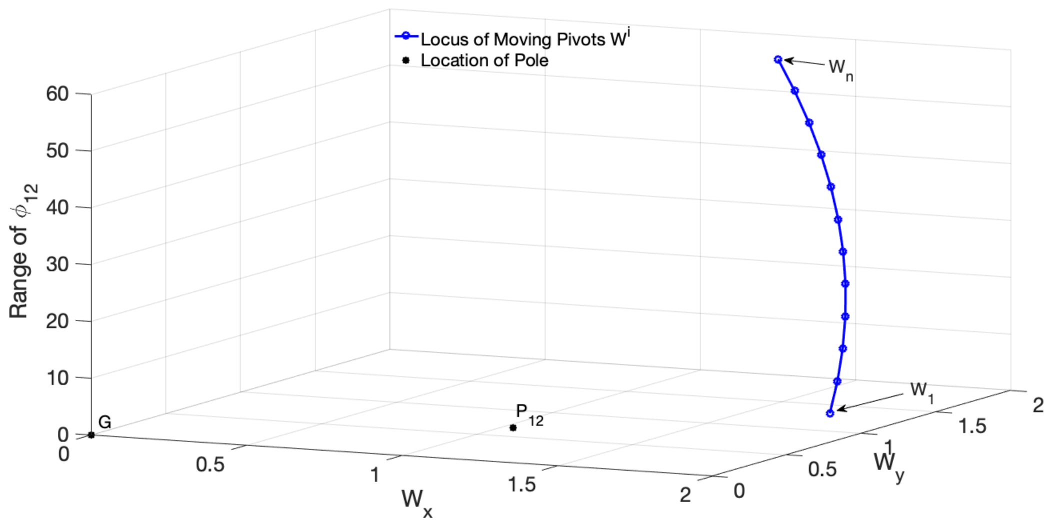


Figure 5.4: Locus of $W^i$ over Pole $P_{12}$

pivot can be obtained using the given conditions. If our link rotates from 0° to 360°, then using the same data i.e pole $P_{12}$, fixed pivot $G$ and initial link position $W^1$ we can obtain the locus of moving pivots $W^n$ at all the instants. This is shown in Figure 5.5,

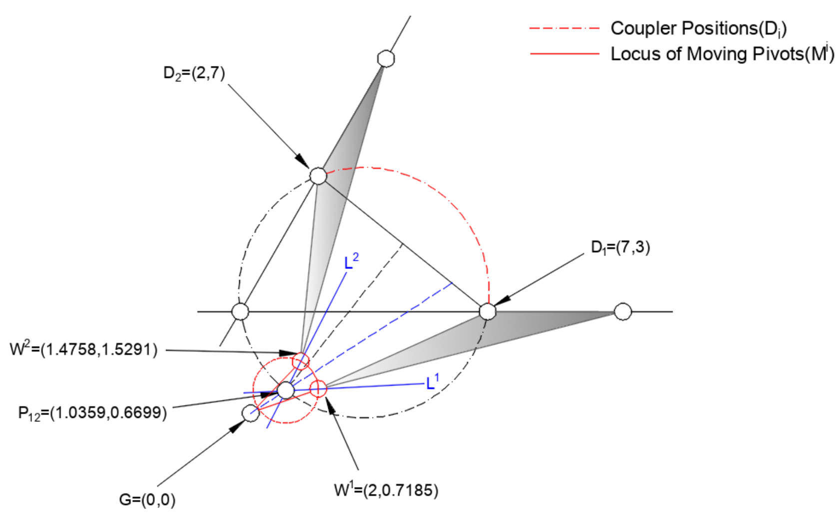


Figure 5.5: Two Position Graphical Representation

The red solid circle as shown represents the locus of moving pivots, and the dashed circle which passes through coupler positions represents the locus of coupler positions. The range of solutions obtained gives the designer a better and faster perspective of Pole positions to be reached.

## 5.2 Three Position Method Results

Similar to two position design, three position design was also carried out for various problems by conventional, Pole and Angle Based and Graphical method using the design approaches given in previous chapters. The solution and their comparison are provided in the following section. One three position design problem solution is shown to understand the results obtained from all three methods.

Consider an initial positions of coupler as $D_1 = 0i + 8j$, second position as $D_2 = 7i + 4j$ and third position as $D_3 = 1i + 6j$. In the problem, rotation from first position to second position is given as $30°$ and rotation from first position to third position is given as $60°$. Now, we evaluate the location of moving pivots for all the three positions. In this problem, the fixed pivot position is considered to be at origin i.e. (0,0) as a free choice. The same problem is solved using Pole and angle based methods using Matlab by method discussed in previous chapter by McCarthy [13]. Also, it is solved by using conventional link design methods by Norton [30]. The comparison of results obtained from all the three methods are accurate as shown in the following Table 5.2,

| | Location of Moving Pivot W1 | Location of Moving Pivot W2 | Location of Moving Pivot W3 |
|---|---|---|---|
| Graphical Method | (-3.65,-6.25) | (0.04,-7.25) | (0.59,-7.22) |
| Analytical Method | (-3.6515,-6.2528) | (0.0359,-7.2408) | (0.5893,-7.2169) |
| Pole And Angle Based Method | (-3.6515,-6.2528) | (0.0359,-7.2408) | (0.5893,-7.2169) |

Table 5.2: Comparison of Solutions from Graphical, Analytical and Pole and Angle Based Methods for Three Position Problem

From a pole position we can reach all the solutions for the angles that we want to reach. Let us assume here that our link rotates following the Grashof's criteria [31], and our crank rotates by an angle of $\phi_{12}$ from position one to two and by an angle of $\phi_{13}$ from position one to three. Hence to reach from position two to three, our crank rotates by an angle of $\phi_{23} = \phi_{13} - \phi_{12}$ about the pole $P_{23}$. We know that the angle between initial and final location of moving pivot about any pole is equal to the phase angle $\phi$. Hence using the assumed location of fixed pivot, angle of rotation and already calculated Pole locations $P'_{ij}s$, we can find the location of all the points that our link reaches using that pole location. Using the following range of variables for phase angles $\phi$:

$$\phi_{12}= 5°, 10°, \ldots, 60°,$$

$$\phi_{13}= 5°, 10°, \ldots, 60°,$$

As the phase angle $\phi$ increases, the moving pivot $W^i$ is observed to rotate from $W^1$ to $W^n$ about the pole $P_{12}$ which is calculated to be as $(0.0359, 0.1340)$, about pole $P_{13}$ which is calculated to be $(-0.6962, -3.0622)$ to third position. Along with that the moving pivot rotates from $W^2$ to $W^n$ about the pole $P_{23} = (0.2679, -6.1952)$.

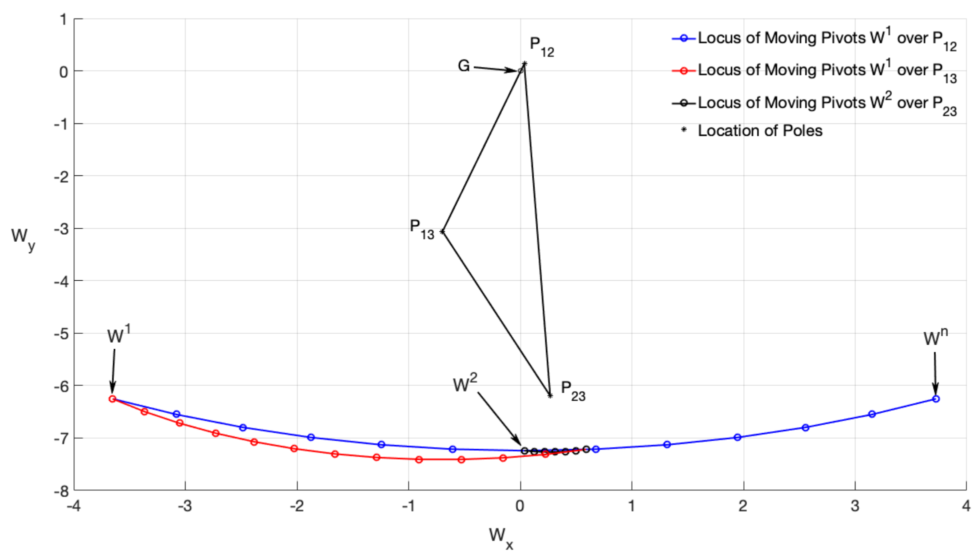


Figure 5.6: Locus of Moving Pivot $W^x$ and $W^y$ over Pole $P_{ij}$

The abscissa is in Figure 5.6 represents the $X$ co-ordinate of the moving pivot $W^i$ and ordinate represents the $Y$ co-ordinate of moving pivot $W^i$. The blue line indicates the locus of moving pivots $W$ over the pole $P_{12}$, the red line represents the locus of moving pivot $W$ over pole $P_{13}$ and black line represents the locus of moving pivot $W$ over pole $P_{23}$. From the output it is observed that the moving pivot $W^i$ rotates around fixed pivot $G$ with a constant link length where $W^1$ is the initial position and $W^n$ is the position of moving pivot at the location we want our coupler to rotate upto.

The abscissa is in Figure 5.7 represents the $X$ co-ordinate of moving pivot $W^i$ and ordinate represents the phase angle $\phi_{12}$. The blue, red and black lines indicates the locus

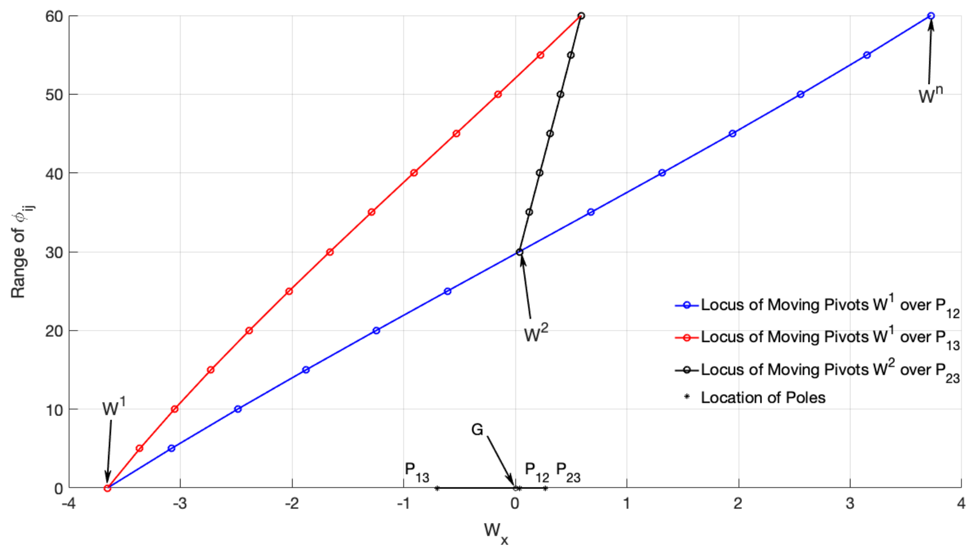


Figure 5.7: Locus of $X$ co-ordinate of Moving Pivot $W^x$ over Pole $P_{ij}$

of moving pivots $W^i$ over the respective pole positions $P_{ij}$.

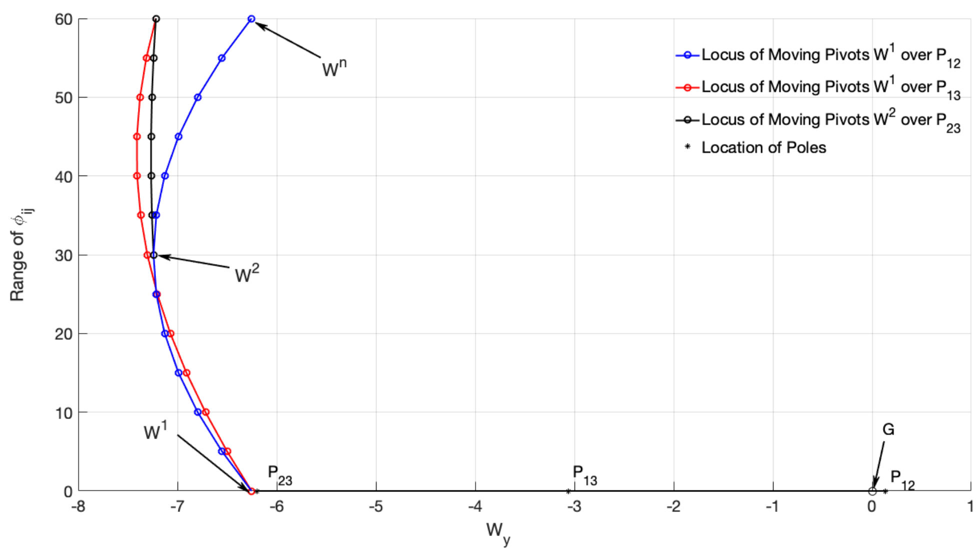


Figure 5.8: Locus of $Y$ co-ordinate of Moving Pivot $W^y$ over Pole $P_{ij}$

The abscissa is in Figure 5.8 represents the $Y$ co-ordinate of moving pivot $W^i$ and ordinate represents the phase angle $\phi_{ij}$.

$X$-axis on the Figure 5.9 represents the $X$ co-ordinates of moving pivot, $Y$-axis represents $Y$ co-ordinate of moving pivot and $Z$-axis represents the increase in phase angle defined in the problem. The triangle formed using all the three pole positions, $P_{12}$, $P_{13}$ and $P_{23}$ is called the Pole Triangle.

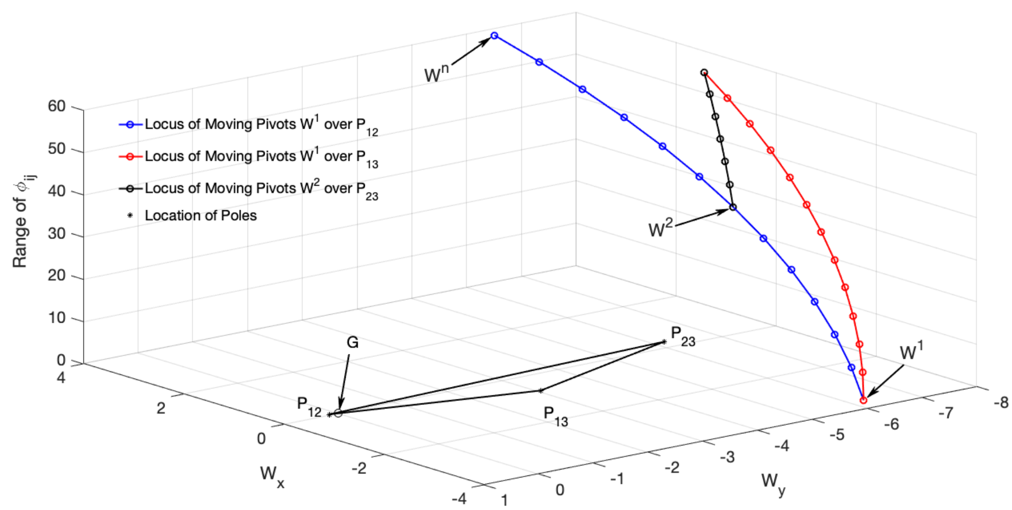


Figure 5.9: Locus of $W^i$ over Pole $P_{ij}$

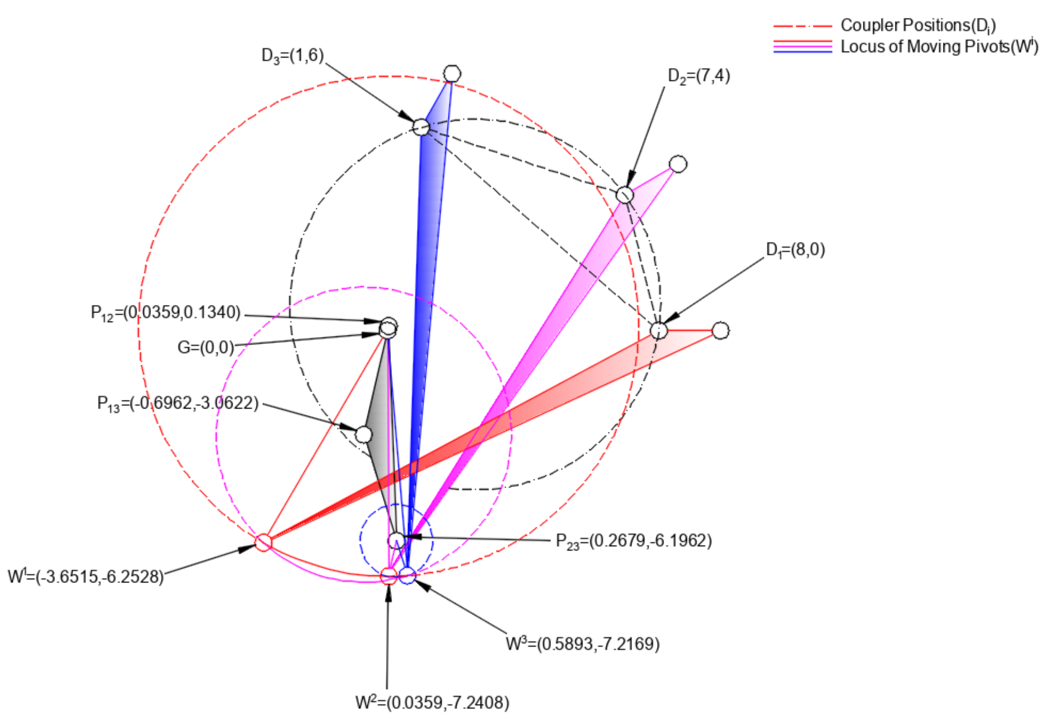


Figure 5.10: Three Position Graphical Representation

The pole triangle provides a geometric way to determine the rotation angle and pole of a displacement $T_{13}$, given the rotation angles$\phi_{ij}$ and poles of two relative displacements $T_{12}$ and $T_{23}$. From the plots it is observed that moving pivot rotates around fixed pivot with a constant link length about the pole $P_{ij}$. Using the pole, all the values of moving pivot can be obtained using the given conditions.

If our link rotates from $0°$ to $360°$, then using the same data i.e pole $P_{ij}$, fixed pivot $G$ and initial link position $W^1$ we can obtain the locus of moving pivots $W^n$ at all the instants. This is shown in Figure 5.10. The red circle as shown represents the locus of moving pivot $W$ over $P_{12}$ for $360°$ rotation of the coupler. Similarly the blue and magenta circle represents locus of moving pivot $W$ over respective poles $P_{23}$ and $P_{13}$. The dashed circle which passes through coupler positions represents the locus of coupler positions. The gray shaded area is the pole triangle. The range of solutions obtained gives the designer a better and faster perspective of Pole positions to be reached.

## 5.3 Four Position Method Results

The four position design of various problems are carried out by conventional method, Pole and Angle Based and Graphical method discussed in previous chapters. The solution and their comparison are provided in the following section. One three position design problem solution is shown to understand the results obtained from all three methods.

Consider an initial positions of coupler as $D_1 = 12i+3j$, second position as $D_2 = 7i+7j$, third position as $D_3 = 4i+9j$ and fourth position as $D_4 = 2i+7j$. In the problem, rotation from first position to second position is given as $30°$, rotation from first position to third position is given as $60°$ and rotation from first position to fourth position is given as $90°$. Now, we evaluate the location of moving pivots for all the four positions using all the methods described in previous chapters.

In this problem, $X$ co-ordinate of fixed pivot is assumed to be zero as a free choice and $Y$ co-ordinate is calculated. $Y$ co-ordinate can be assumed and calculations can be carried out on $X$ co-ordinate as well. There are various ways of calculating $y$ variable of a cubic equation, out of which Brute-Force method [32] is used. Then evaluated value of y-coordinate is used to calculate poles and locations of moving pivots.

The same problem is solved using Pole and Angle based method using Matlab by using four position design method mentioned in previous chapter by McCarthy [13]. Similar to two and three position approaches, four position design is also carried out using conventional method as given in Norton [30]. The comparison of results obtained from all the three methods are accurate as shown in the following Table 5.3,

| | Location of Moving Pivot W1 | Location of Moving Pivot W2 | Location of Moving Pivot W3 | Location of Moving Pivot W4 |
|---|---|---|---|---|
| Graphical Method | (2.26,16.87) | (-8.37,14.14) | (-12.86,7.5) | (-11.97,-2.73) |
| Analytical Method | (2.26,16.8703) | (-8.37,14.1422) | (-12.8619,7.50) | (-11.9703,-2.7307) |
| Pole & Angle Based Method | (2.26,16.8703) | (-8.37,14.1422) | (-12.8619,7.50) | (-11.9703,-2.7307) |

Table 5.3: Comparison of Solutions from Graphical, Analytical and Pole and Angle Based Methods for Four Position Problem

From a pole position we can reach all the solutions for the angles that we want to reach. Same assumption which is considered in two and three position problems, is considered here, that our link rotates following the Grashof's criteria [31], and our crank rotates by an angle of $\phi_{12}$ from position one to two, an angle of $\phi_{13}$ from position one to three and by an angle of $\phi_{14}$ from position one to four. Hence to reach from position two to three, our crank rotates by an angle of $\phi_{23} = \phi_{13} - \phi_{12}$ about the pole $P_{23}$ and to reach from position three to four our crank rotates by an angle of $\phi_{34} = \phi_{14} - \phi_{13}$ about the pole $P_{34}$. We know that the angle between initial and final location of moving pivot about any pole is equal to the phase angle $\phi$. Hence using the assumed location of fixed pivot, angle of rotation and already calculated Pole locations $P'_{ij}s$, we can find the location of all the points that our link reaches using that pole location.

Using the following range of variables for phase angles $\phi$:

$$\phi_{12} = 10^\circ, 20^\circ, \ldots, 100^\circ,$$

$$\phi_{13} = 10^\circ, 20^\circ, \ldots, 110^\circ,$$

$$\phi_{14} = 10^\circ, 20^\circ, \ldots, 120^\circ,$$

As the phase angle $\phi$ increases, the moving pivot $W^i$ is observed to rotate from $W^1$ to $W^n$ about the pole $P_{12}$ which is calculated to be as $(2.0359, -4.3301)$ to second position, about pole $P_{13}$ which is calculated to be $(2.8038, -0.9282)$ to third position and about the pole $P_{14}$ which is calculated to be $(5, 0)$ to fourth position. Along with that the moving pivot rotates from $W^2$ to $W^3$ about the pole $P_{23} = (1.7679, 2.4019)$. The moving pivot rotates from $W^3$ to $W^4$ about pole $P_{34} = (6.7321, 4.2679)$.

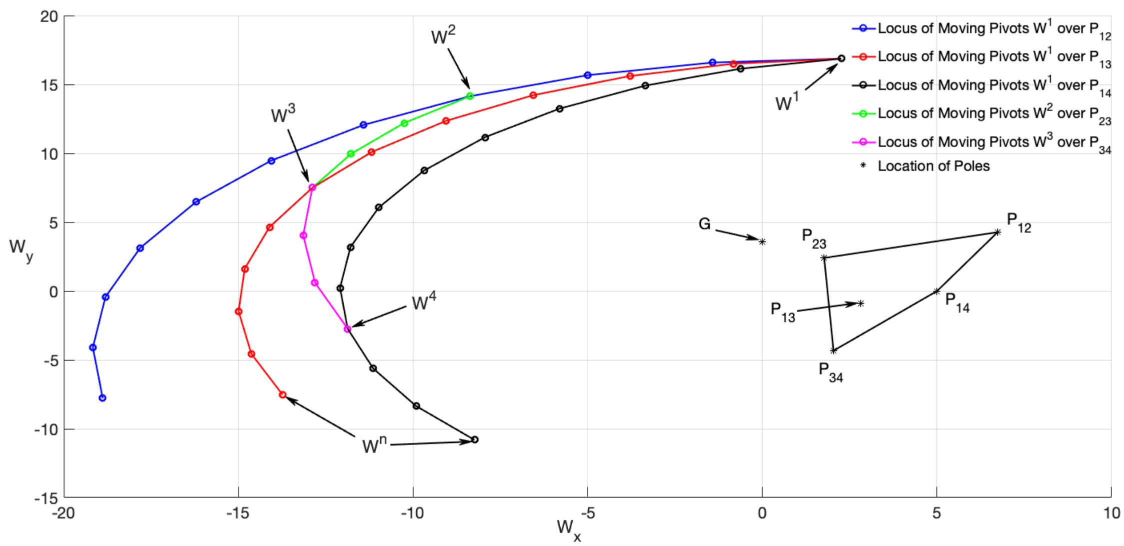


Figure 5.11: Locus of Moving Pivot $W^x$ and $W^y$ over Pole $P_{ij}$

The abscissa is in Figure 5.11 represents the $X$ co-ordinate of the moving pivot $W^i$ and ordinate represents the $Y$ co-ordinate of moving pivot $W^i$. The blue line indicates the locus of moving pivots $W$ over the pole $P_{12}$, the red line represents the locus of moving pivot $W$ over pole $P_{13}$, black line represents the locus of moving pivot $W$ over pole $P_{14}$, green line represents the locus of moving pivot $W$ over pole $P_{23}$ and magenta line represents the locus of moving pivot $W$ over pole $P_{34}$. From the output it is observed that the moving pivot $W^i$ rotates around fixed pivot $G$ with a constant link length where $W^1$ is the initial position and $W^n$ is the position of moving pivot at the location we want our coupler to rotate upto.

The abscissa is in Figure 5.12 represents the $X$ co-ordinate of moving pivot $W^i$ and ordinate represents the phase angle $\phi_{12}$. The blue, red, black, green and magenta lines indicates the locus of moving pivots $W^i$ over the respective pole positions $P_{ij}$.

The abscissa is in Figure 5.13 represents the $Y$ co-ordinate of moving pivot $W^i$ and

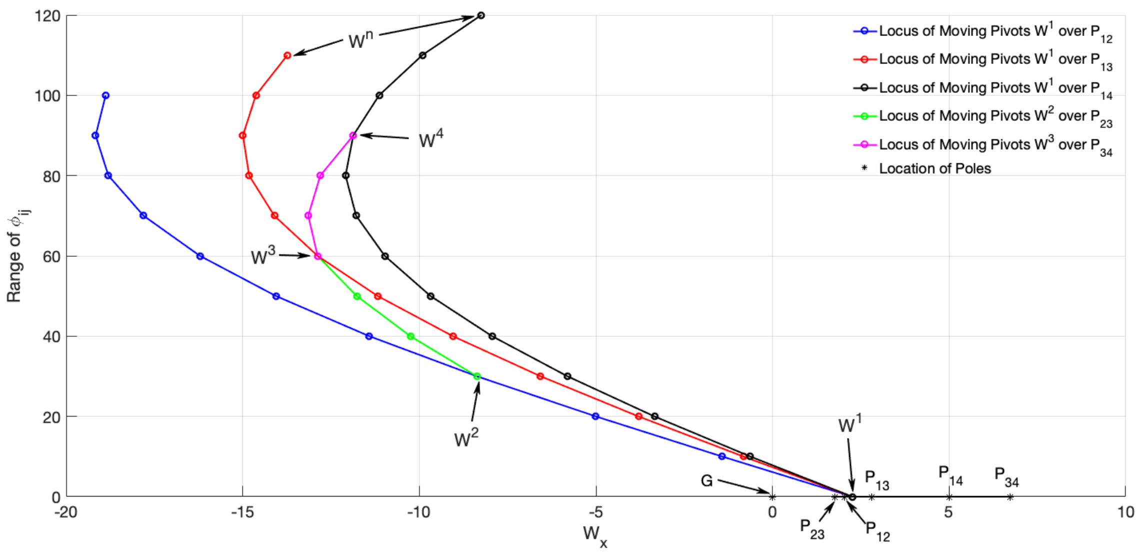


Figure 5.12: Locus of $X$ co-ordinate of Moving Pivot $W^x$ over Pole $P_{ij}$

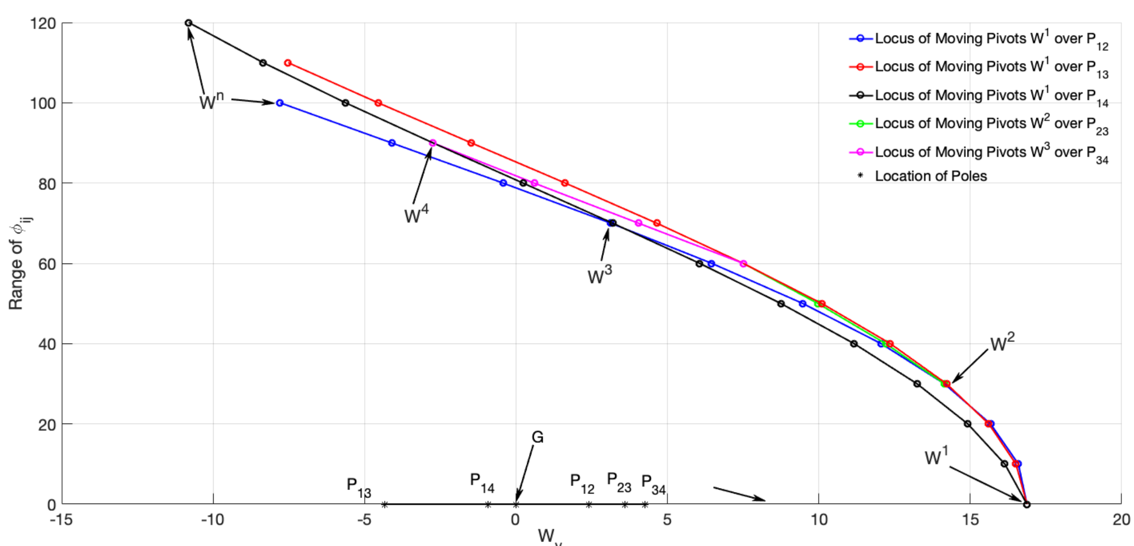


Figure 5.13: Locus of $Y$ co-ordinate of Moving Pivot $W^y$ over Pole $P_{ij}$

ordinate represents the phase angle $\phi_{ij}$.

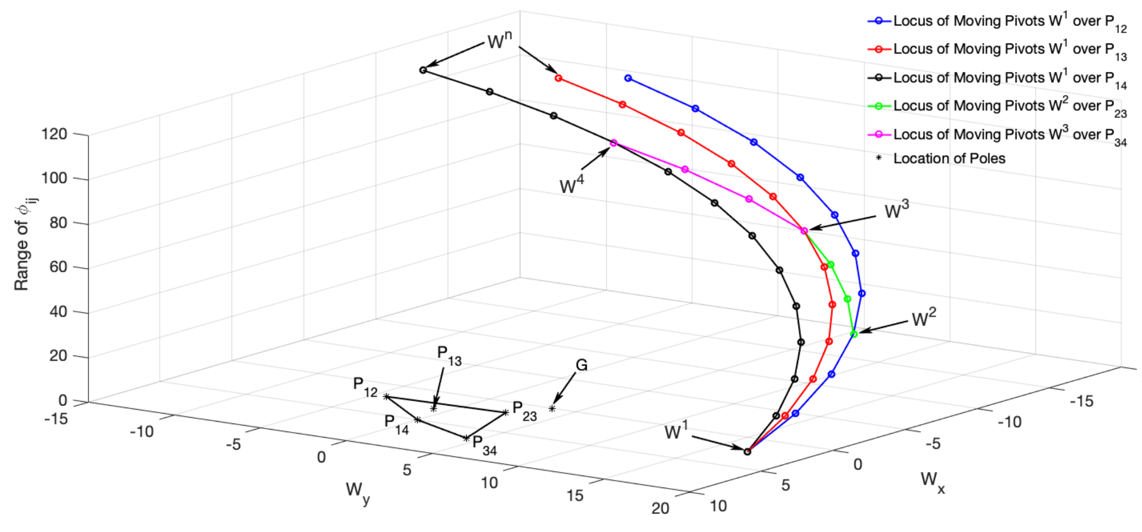


Figure 5.14: Locus of $W^i$ over Pole $P_{ij}$

$X$-axis on the Figure 5.14 represents the $X$ co-ordinates of moving pivot, $Y$-axis represents y co-ordinate of moving pivot and $Z$-axis represents the increase in phase angle defined in the problem. The quadrilateral formed using all the three pole positions, $P_{12}$, $P_{23}$, $P_{34}$ and $P_{14}$ is called the Pole Quadrilateral formed according to Brumester's Theorem [6].

The pole quadrilateral provides a geometric way to determine the rotation angle and pole of a displacement $T_{14}$, given the rotation angles$\phi_{ij}$ and poles of two relative displacements $T_{12}$, $T_{23}$ and $T_{34}$. From the plots it is observed that moving pivot rotates around fixed pivot with a constant link length about the pole $P_{ij}$. Once a center point is obtained by this construction, any three of the four positions can be used to construct the associated moving pivot. The result is an RR chain that reaches the four specified positions. Notice that for a given increment of rotation of the crank $P_{12}P_{23}$ of the opposite pole quadrilateral there are actually two center points, one for each assembly of the quadrilateral as a linkage. The relative poles obtained from all of the configurations of the opposite-pole quadrilateral form a cubic curve known as the center-point curve. Using the pole, all the values of moving pivot can be obtained using the given conditions.

If our link rotates from 0° to 360°, then using the same data i.e poles $P'_{ij}s$, fixed pivot

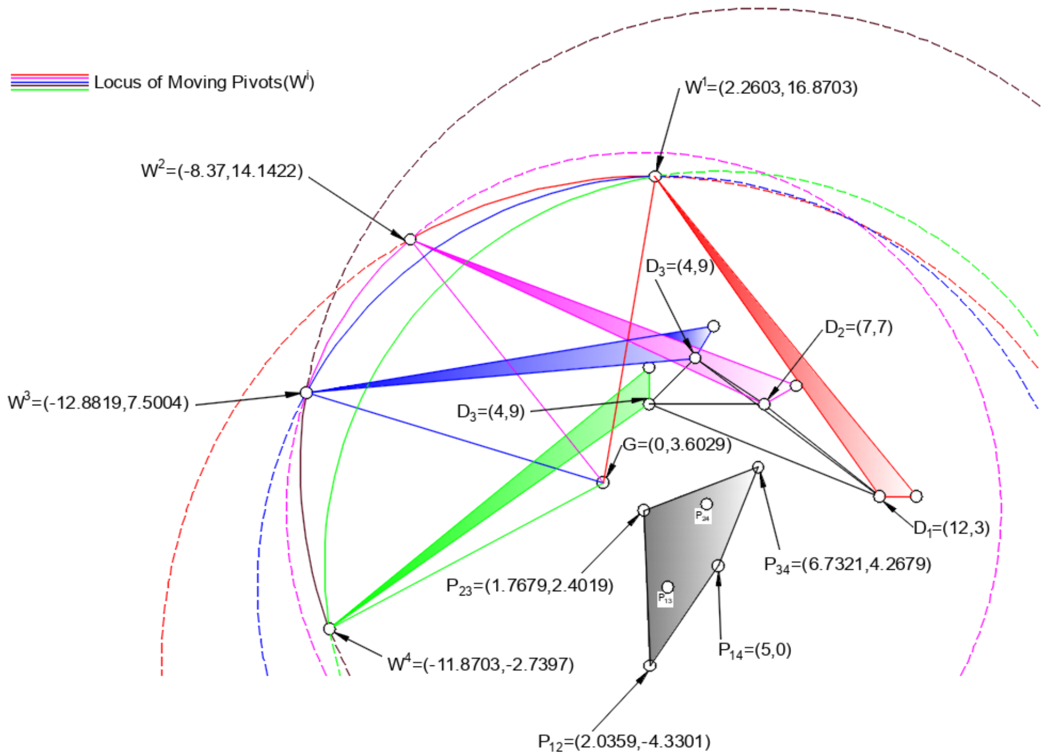


Figure 5.15: Four Position Graphical Representation

$G$ and initial link position $W^1$ we can obtain the locus of moving pivots $W^n$ at all the instants. This is shown in Figure 5.10. The red circle as shown represents the locus of moving pivot $W$ over $P_{12}$ for 360° rotation of the coupler. Similarly blue, green, magenta and maroon circle represents locus of moving pivot $W$ over respective poles $P_{13}$, $P_{14}$, $P_{23}$ and $P_{34}$. The dashed circle which passes through coupler positions represents the locus of coupler positions. The gray shaded area is the pole quadrilateral. The range of solutions obtained gives the designer a better and faster perspective of Pole positions to be reached.

All the results obtained from all the methods are to show that moving pivots can be obtained by calculating the pole positions from the given coupler positions to be reached. By assuming the fixed pivot, the designer can analyze the moving pivots just from the pole calculations. This gives the designer a better and faster approach to design a link and hence a mechanism.

From the examples explained above, the primary focus is to emphasize the importance of poles in the design. Poles give more information about the design of linkage or mechanism to the designer and provides with the variation of solutions that can be determined. Pole and Angle Based Method also gives a graphical tool of design. All of which, provides designer a better perspective to observe a pattern in the design of a specific mechanism rather than doing a blind analysis carried out by conventional methods which is a trial and error approach.

# Chapter 6

# Conclusion

In this work, an algorithm for designing a linkage for two position, three position and four position problems with respect to Pole and Angle based design method was developed and codified in MatLab. In Matlab, the designer can express the numerical values to a precision over ten decimal places. All calculated linkage dimensions are dimension less. All the data calculated on Matlab for linkage is specified to four decimal places. The data calculated for graphical design method is specified to two decimal places. Coordinate systems with X,Y and Z labels for respective axis are specified throughout this work.

As written, the algorithm developed and codified in this work basically takes the input to the defined problem and solves the design problem with respect to pole positions. The designed problems defined in the sections are used to demonstrate the importance of Pole and pole location through this work. The significance of Pole and Angle Based Method can be determined using this work. In real-world engineering design, the linkages and hence mechanisms are designed either by using conventional design methods or Graphical Methods. Either of those, makes designer's work more tedious as for each specified angular position, the design has to be reevaluated. Though this work, the significance of poles can be understood. Using those pole positions, a designer can visualize all the locations that the link reaches to and hence decide the changes that has to be made.

Although the algorithm presented in this work was codified in Matlab, the designer is not necessarily limited to Matlab. The designer can codify the algorithm presented in this work in other platforms such as C, C++, MathCAD, Mathematica, Maple, etc that are well suited for computationally intense calculations required in the algorithm.

Solving different examples using Pole and Angle based method by McCarthy [13], the study is focused on importance of poles in the design of linkages and mechanism. The pole location changes with change in problem definition. Hence, for a defined problem, the pole location is fixed which means the designer can evaluate a number of designs by altering fixed pivot $G$ positions, altering the phase angle that our mechanism rotates to. Pole and Angle based approach also can be used if the designer wants to evaluate the problem by having a fixed location of $G$ and variable precision point locations. All of the above variations can be evaluated just on the basis of pole positions within short time frame.

For a series of prescribed rigid body positions, an infinite number of planar solutions exist. Sorting through the unlimited number of possible solutions to find one that ensures full link rotatability, satisfies feasible phase angles and is as compact as possible is overwhelming given a set of positions. In this work, the algorithm is presented by which a designer can select optimum design of linkage from the moving pivot curves obtained from the specified problem.

# Chapter 7

# Future Scope

The design of another RR linkage for a four-bar mechanism can be carried out using the Pole and Angle Based approach. Combining the results from both the link designs, a four bar mechanism can be designed. The current work gives a general algorithm for linkage design, a similar approach can be used to design a PR linkage and can be evaluated. Although conventional design approaches are used for most of mechanism designs, pole and angle based design can be used to design all the mechanisms giving any designer an easier and faster perspective to mechanism design. A similar approach can be used to design five, six or eight bar mechanisms as well.

# Appendix A

## Two Position Synthesis Using Pole and Angle Based Method

```
%Two Position Synthesis by Pole and Angle Based Method

%Couper Points D1 and D2
D1 = [7 3]' ;
D2 = [2 7]' ;

m=60; %Number of iterations

%Defining array of Positions, Poles and Rotation Matrices
P_1=[];
W_1=[];
W_2=[];

ph_1=[];

%Iterative loop
for phi=5:5:m

cc = cosd(phi);
ss = sind(phi);
A = [ cc, -ss;
      ss ,cc ] ; %Calculated Rotation Matrices
t=phi;
```

```
d = D2 - A*D1; %Displacement
ph_1=[ph_1 t];
p12 = inv( eye(2) - A)*d; % Calculated pole location
P_1=[P_1 p12];

%select G and lambda as free choices
p = p12(1);
q = p12(2);

x = 0;
y = 0;
lam = 2; % select origin at zero (arbitrary)
%selection of lambda is also arbitrary choose as first position - 3
G(1)=x;
G(2)=y;
AA = ((cc - 1)*(x - p)) + (ss*(y - q)); %Defining constants
B = -ss*(x - p) + (cc-1)*(y-q);
C = (cc-1)* (p*(x-p) + q*(y-q)) + ss*(p*y - q*x);
mu = (C - AA*lam)/B;
W1 =[lam mu]';
W_1=[W_1 W1]; %Calculated Moving Pivots

W2 = p12 + A*(W1-p12);
W_2=[W_2 W2];
end

W_21=[];
W11 = W_1(:,length(W_1));

for pp=5:5:m
```

```
cc1 = cosd(pp);
ss1 = sind(pp);
A1 = [ cc1, -ss1;
      ss1 ,cc1 ] ;
p1=P_1(1,12);
q1=P_1(2,12);
W= W11-p12;
W21 = p12 + A1*W;
W_21=[W_21 W21];
end

figure(1)
plot3(W_21(1,:),W_21(2,:),ph_1,'b-o')
grid on
hold on
xlabel('W_x')
ylabel('W_y')
zlabel('Range of \phi_{12}')
title('Locus of Moving Pivot W^i over Pole P_{12}')
plot(p12(1,1),p12(2,1),'k*'); hold on
text(p12(1,1)+0.005,p12(2,1)+0.005,2,'P_{12}',
'Color','black','FontSize',10)
plot(G(1,1),G(1,2),'k*'); hold on
text(G(1,1)+0.005,G(1,2)+0.005,2,'G','Color','black','FontSize',10)
legend('Locus of Moving Pivots W^i','Location of Pole')
```

# Appendix B

# Three Position Synthesis Using Pole and Angle Based Method

```
% Three Position Synthesis by Pole and Angle Based Method


% Coupler positions of D1, D2 and D3
D1=[8;0];
D2=[7;4];
D3=[1;6];


m = 60;             %Defining the range of iterations along i
n = 60;             %Defining the range of iterations along j
W = [];             %Defining initial link length
P_1=[];
P_2=[];
P_3=[];
W_1 =[];
W_x =[];
s = 5;              %Defining the Step
ph12 = zeros(m,n);
ph13 = zeros(m,n);


%Iterative loop
for i=5:s:m
```

```
for j=5:s:n
  k=(i-5)+1;
  l=(j-5)+1;
  % Determining the angles between D1, D2 and D3
  ph12(k,l)=i+(0*j);
  ph13(k,l)=(0*i)+j;
  ph_12=i;
  ph_13=j;
  ph_23 = ph_13-ph_12;

  % Determining the rotation matrix from D1 to D2, D2 to D3 and D1
  A12 = [ cosd(ph_12)  -sind(ph_12);
          sind(ph_12)  cosd(ph_12) ];
  A13 = [ cosd(ph_13)  -sind(ph_13);
          sind(ph_13)  cosd(ph_13) ];
  A23 = [ cosd(ph_23)   -sind(ph_23);
          sind(ph_23)   cosd(ph_23) ]; %Calculating Rotation Matrices

  % Translation from W1 to W2=d12, W2 to W3=d23 and W1 to W3=d13
  d12 = D2-(A12*D1);
  d13 = D3-(A13*D1);
  d23 = D3-(A23*D2);

  % Finding the poles P12, P13 and P23
  P12 = inv(eye(2)-A12)*d12;
  P13 = inv(eye(2)-A13)*d13;
  P23 = inv(eye(2)-A23)*d23;
  P_1=[P_1 P12];
  P_2=[P_2 P13];
  P_3=[P_3 P23];
```

```
% Defining variables to poles and angles
c2 = cosd(ph_12);
s2 = sind(ph_12);
c3 = cosd(ph_13);
s3 = sind(ph_13);
p2 = P12(1);
q2 = P12(2);
p3 = P13(1);
q3 = P13(2);

% Determining the fixed pivot G as free choice
G=[0,0];

% Finding the coefficients of lambda and mu
A2 = ((c2-1) * (G(1)-p2))   +   (s2 * (G(2)-q2));
B2 = (-s2*(G(1)-p2))  +  ((c2-1)*(G(2)-q2));
C2 = ((c2-1)* (p2*(G(1)-p2) + q2 *(G(2)-q2)))+s2*(p2*G(2)-q2*G(1));
A3 = (c3-1)*(G(1)-p3)+s3*(G(2)-q3);
B3 = -s3*(G(1)-p3)+(c3-1)*(G(2)-q3);
C3 = (c3-1)*(p3*(G(1)-p3)+q3*(G(2)-q3))+s3*(p3*G(2)-q3*G(1));

% Matrix of coefficients
AA = [A2  B2 ;
      A3  B3];
CC = [C2;
      C3];

% Finding lambda and mu i.e. W1, W2 and W3
W1 = (inv(AA))*CC;
W2 = P12 + (A12*(W1-P12));
```

```
    W3 = P13 + (A13*(W1-P13));
    W_1=[W_1 W1];
    W_x=[W_x W2];

  end

end

P_12  =  P_1(:, 1:12:end);
p=P_12(:,6);
W_2 = [W_1(:,72)];
W11 = W_1(:,72);

 for pp=5:5:m

    cc1 = cosd(pp);
    ss1 = sind(pp);
    A1 = [ cc1, -ss1;
           ss1 ,cc1 ] ;
    p1=P_1(1,12);
    q1=P_1(2,12);
    W= W11-p;
    W21 = p + A1*W;
    W_2=[W_2 W21];

 end

p_12  =  ph12(1:s:end, 1:s:(end-s));   %Angle matrix for ph12
p_13  =  ph13(1:s:end, 1:s:(end-s));   %Angle matrix for ph13
```

```
P_13  =  P_2(:, 1:1:12);
po=P_13(:,12);
W_o = [W_1(:,72)];
Wo1 = W_1(:,72);

 for pp1=5:5:n

     cc2 = cosd(pp1);
     ss2 = sind(pp1);
     A2 = [ cc2, -ss2;
            ss2 ,cc2 ] ;
     W= Wo1-po;
     Wn1 = po + A2*W;
     W_o=[W_o Wn1];

 end

P_23  =  P_3(:, 1:1:12);
pn=P_23(:,7);
W_n = [W_x(:,72)];
Wn_1 = W_x(:,72);

 for p_n=5:5:30

     cc2 = cosd(p_n);
     ss2 = sind(p_n);
     A11 = [ cc2, -ss2;
            ss2 ,cc2 ] ;
     Wn= Wn_1-pn;
     Wnn1 = pn + A11*Wn;
```

```
    W_n=[W_n Wnn1];

 end

x=30:5:60;
p12=0:5:60;
figure(1)
plot3(W_2(1,:),W_2(2,:),p12,'b-o'); hold on
plot3(W_o(1,:),W_o(2,:),p12,'r-o'); hold on
plot3(W_n(1,:),W_n(2,:),x,'k-o'); hold on
grid on
xlabel('W_x')
ylabel('W_y')
zlabel('Range of \phi_{ij}')
title('Locus of Moving Pivot W^i over Pole P_{12}')
plot(p(1,1),p(2,1),'k*'); hold on
text(p(1,1)+.2,p(2,1)+.2,2,'P_{12}','Color','black','FontSize',10)
plot(po(1,1),po(2,1),'k*'); hold on
text(po(1,1)-.2,po(2,1)-.2,2,'P_{13}','Color','black')
plot(pn(1,1),pn(2,1),'k*'); hold on
text(pn(1,1)+.2,pn(2,1)+.2,2,'P_{23}','Color','black')
plot(G(1,1),G(1,2),'ko'); hold on
text(G(1,1)+.2,G(1,2)+.2,2,'G','Color','black')
plot([p(1,1),po(1,1)],[p(2,1),po(2,1)],'k-')
plot([pn(1,1),po(1,1)],[pn(2,1),po(2,1)],'k-')
plot([p(1,1),pn(1,1)],[p(2,1),pn(2,1)],'k-')
legend('Locus of Moving Pivots W^1 over P_{12}',
'Locus of Moving Pivots W^1 over P_{13}',
'Locus of Moving Pivots W^2 over P_{23}',
'Location of Poles')
```

# Appendix C

# Four Position Synthesis Using Pole and Angle Based Method

```
% Four Position Design Using Poles

% Coupler positions of D1, D2, D3 and D4
D1 = [12 3]';
D2 = [7 7]';
D3 = [4 9]';
D4 = [2 7]';

% Orientations of end point
ph12 = 30;
ph13 = 60;
ph14 = 90;
ph23 = ph13-ph12;
ph34 = ph14-ph13;

% Calculating Rotation Matrices

A12 = [ cosd(ph12) -sind(ph12) ;
        sind(ph12) cosd(ph12)  ];
A13 = [ cosd(ph13) -sind(ph13) ;
        sind(ph13) cosd(ph13)  ];
A14 = [ cosd(ph14) -sind(ph14) ;
        sind(ph14) cosd(ph14)  ];
```

```
A23 = [ cosd(ph23) -sind(ph23) ;
        sind(ph23) cosd(ph23)  ];
A34 = [ cosd(ph34) -sind(ph34) ;
        sind(ph34) cosd(ph34)  ];

% Translation dij,i<j

d12 = D2 - A12*D1;
d13 = D3 - A13*D1;
d14 = D4 - A14*D1;
d23 = D3 - A23*D2;
d34 = D4 - A34*D3;

% Calculation of poles

P12 = (eye(2) - A12)\d12;
P13 = (eye(2) - A13)\d13;
P14 = (eye(2) - A14)\d14;
P23 = (eye(2) - A23)\d23;
P34 = (eye(2) - A34)\d34;

% Symbolic notation for all angles
c2 = cosd(ph12);  s2 = sind(ph12);
c3 = cosd(ph13);  s3 = sind(ph13);
c4 = cosd(ph14);  s4 = sind(ph14);
c5 = cosd(ph23);  s5 = sind(ph23);
c6 = cosd(ph34);  s6 = sind(ph34);

% Symbolic notation for all pole positions
p2 = P12(1);  q2 = P12(2);
```

```
p3 = P13(1);  q3 = P13(2);
p4 = P14(1);  q4 = P14(2);
p5 = P23(1);  q5 = P23(2);
p6 = P34(1);  q6 = P34(2);

% x and y are locations of fixed pivot G
% Define symbolic characters syms x, syms y
% Continue on to design problem - Given G find W1
% First select x as free choice
x=0;
% Solve for second coordinate y
% This program does it by trial and error using Brute Force Method
% Ordinarily, one can also solve this part using fsolve or another way
% Next define symbolic characters
% syms x, use syms x if you are selecting y coordinate of G as free choice
syms y
% For 2nd position
AA2 = (c2 -1)*(x-p2) + s2*(y-q2);
BB2 = -s2*(x-p2) +(c2-1)*(y-q2);
CC2 = (c2-1)*(p2*(x-p2) + q2*(y-q2) )  + s2*(p2*y - q2*x);
% For 3rd position
AA3 = (c3 -1)*(x-p3) + s3*(y-q3);
BB3 = -s3*(x-p3) +(c3-1)*(y-q3);
CC3 = (c3-1)*(p3*(x-p3) + q3*(y-q3) )  + s3*(p3*y - q3*x);
% For 4th position
AA4 = (c4 -1)*(x-p4) + s4*(y-q4);
BB4 = -s4*(x-p4) +(c4-1)*(y-q4);
CC4 = (c4-1)*(p4*(x-p4) + q4*(y-q4) )  + s4*(p4*y - q4*x);
% Define matrix M
MM = [ AA2 BB2 CC2 ;
```

```
       AA3 BB3 CC3 ;
       AA4 BB4 CC4 ];

% Center Point Equation is given by Determinant of M
curve = det(MM);
% Set the Curve Equation to Zero for matrix M to be of Rank 2
eqn = curve == 0;
% Solution of cubic center point equation
sol =  solve(eqn,y);
% The next step will check to check the number of solutions
% This operation writes the solution in double precision
sol2 = double(sol);
% It turns out that the det = 0 equation has three solutions, one real and
% two complex. We identify the real solution as the first and eliminate
% complex solutions as link does not have a complex coordinate solution

y = double(sol(1)); % Identify the Real value of y to use

m = 100;        %Defining the range of iterations along ph12
n = 110;        %Defining the range of iterations along ph13
o = 120;        %Defining the range of iterations along ph14

s = 10;         %Defining the Step Variation of phase angle
ph12 = zeros(m,n,o);
ph13 = zeros(m,n,o);
ph14 = zeros(m,n,o);
P_12 = [];
P_13 = [];
P_14 = [];
P_23 = [];
```

```
P_34 = [];
W_1_1= [];
W_2_1= [];
W_3_1= [];
W_4_1= [];

for i=10:s:m

    for j=20:s:n

        for p=30:s:o

        k=(i-10)+1;
        l=(j-20)+1;
        q=(p-30)+1;

        % Determining the angles between D1, D2 and D3
        ph12(k,l,q)=i;
        ph13(k,l,q)=j;
        ph14(k,l,q)=p;
        ph_12=i;
        ph_13=j;
        ph_14=p;
        ph_23 = ph_13-ph_12;
        ph_34 = ph_14-ph_13;

        % Calculation of Rotation Matrix

        A12 = [ cosd(ph_12)  -sind(ph_12) ;
                 sind(ph_12)   cosd(ph_12)  ];
```

```
A13 = [ cosd(ph_13)  -sind(ph_13) ;
             sind(ph_13)   cosd(ph_13)  ];
A14 = [ cosd(ph_14)  -sind(ph_14) ;
             sind(ph_14)   cosd(ph_14)  ];
A23 = [ cosd(ph_23)  -sind(ph_23) ;
             sind(ph_23)   cosd(ph_23)  ];
A34 = [ cosd(ph_34)  -sind(ph_34) ;
             sind(ph_34)   cosd(ph_34)  ];

% Translation
d12 = D2 - A12*D1;
d13 = D3 - A13*D1;
d14 = D4 - A14*D1;
d23 = D3 - A23*D2;
d34 = D4 - A34*D3;

%Calculating poles
P12 = (eye(2) - A12)\d12;
P13 = (eye(2) - A13)\d13;
P14 = (eye(2) - A14)\d14;
P23 = (eye(2) - A23)\d23;
P34 = (eye(2) - A34)\d34;

%Storing Values of Poles
P_12=[P_12 P12];
P_13=[P_13 P13];
P_14=[P_14 P14];
P_23=[P_23 P23];
P_34=[P_34 P34];
```

```
% Symbolic Notation for angles
c2 = cosd(ph_12);   s2 = sind(ph_12);
c3 = cosd(ph_13);   s3 = sind(ph_13);
c4 = cosd(ph_14);   s4 = sind(ph_14);
c5 = cosd(ph_23);   s5 = sind(ph_23);
c6 = cosd(ph_34);   s6 = sind(ph_34);

% Symbolic Notation for Poles
p2 = P12(1);   q2 = P12(2);
p3 = P13(1);   q3 = P13(2);
p4 = P14(1);   q4 = P14(2);
p5 = P23(1);   q5 = P23(2);
p6 = P34(1);   q6 = P34(2);

%Using G obtained from Brute Force Method above
G=[x,y]';
x=G(1);
y=G(2);

% Calculating constants A2 A3 and A4 for all Positions
% For 2nd position
AR2 = (c2 -1)*(x-p2) + s2*(y-q2);
BR2 = -s2*(x-p2) +(c2-1)*(y-q2);
CR2 = (c2-1)*(p2*(x-p2) + q2*(y-q2))  + s2*(p2*y - q2*x);

% For 3rd position
AR3 = (c3 -1)*(x-p3) + s3*(y-q3);
BR3 = -s3*(x-p3) +(c3-1)*(y-q3);
CR3 = (c3-1)*(p3*(x-p3) + q3*(y-q3))  + s3*(p3*y - q3*x);
```

```
        % For fourth position
        AR4 = (c4 -1)*(x-p4) + s4*(y-q4);
        BR4 = -s4*(x-p4) +(c4-1)*(y-q4);
        CR4 = (c4-1)*(p4*(x-p4) + q4*(y-q4))  + s4*(p4*y - q4*x);

        AAA= [ AR2 BR2 ;
                    AR3 BR3 ;
                    AR4 BR4];
        CCC= [ CR2; CR3; CR4];
        W1= (AAA)\CCC;
        W_1_1=[W_1_1 W1];

        % Calculating W2, W3, W4 using the Pole Equation

        W2 = P12 + A12*(W1 - P12);
        W3 = P13 + A13*(W1 - P13);
        W4 = P14 + A14*(W1 - P14);
        W_2_1=[W_2_1  W2];
        W_3_1=[W_3_1  W3];
        W_4_1=[W_4_1  W4];

        end

    end

end

%Matrices for Phase Angles ph_12,ph_13 and ph_14

p_12  =  ph12(1:s:end, 1:s:(end-s), 1:s:(end-(2*s)));
```

```
p_13  =  ph13(1:s:end, 1:s:(end-s), 1:s:(end-(2*s)));

p_14  =  ph14(1:s:end, 1:s:(end-s), 1:s:(end-(2*s)));


%Calculating W_i over respective Poles P_{ij}


Pp_12  =  P_12(:, 1:100:1000);

p_1=Pp_12(:,3);

W_1 = [W_1_1(:,247)];

Wo1 = W_1_1(:,247);


 for pp=10:s:m


     cc1 = cosd(pp);

     ss1 = sind(pp);

     A1 = [ cc1, -ss1;

            ss1 ,cc1 ] ;

     W= Wo1-p_1;

     Wn1 = p_1 + A1*W;

     W_1=[W_1 Wn1];


 end


Pp_13  =  P_13(:, 1:10:100);

p_2=Pp_13(:,5);

W_2 = [W_1_1(:,247)];

Wp1 = W_1_1(:,247);


 for pp1=10:s:n


     cc_1 = cosd(pp1);
```

```
     ss_1 = sind(pp1);
     A1 = [ cc_1, -ss_1;
            ss_1 ,cc_1 ] ;
     W= Wp1-p_2;
     Wn2 = p_2 + A1*W;
     W_2=[W_2 Wn2];

 end

Pp_14  =  P_14(:, 1:1:10);
p_3=Pp_14(:,7);
W_3 = [W_1_1(:,247)];
Wq1 = W_1_1(:,247);

 for pp2=10:s:o


     cc_2 = cosd(pp2);
     ss_2 = sind(pp2);
     A2 = [ cc_2, -ss_2;
            ss_2,  cc_2 ] ;
     W= Wp1-p_3;
     Wn3 = p_3 + A2*W;
     W_3=[W_3 Wn3];

 end

Pp_23  =  P_23(:, 1:10:100);
p_4=Pp_23(:,3);
W_4 = [W_2_1(:,247)];
Wr1 = W_2_1(:,247);
```

```
 for pp3=10:s:30

     cc_3 = cosd(pp3);
     ss_3 = sind(pp3);
     A3 = [ cc_3, -ss_3;
            ss_3,  cc_3 ] ;
     W= Wr1-p_4;
     Wn4 = p_4 + A3*W;
     W_4=[W_4 Wn4];

 end

Pp_34  =  P_34(:, 1:1:10);
p_5=Pp_34(:,3);
W_5 = [W_3_1(:,247)];
Ws1 = W_3_1(:,247);

 for pp4=10:s:30

     cc_4 = cosd(pp4);
     ss_4 = sind(pp4);
     A4 = [ cc_4, -ss_4;
            ss_4,  cc_4 ] ;
     W= Ws1-p_5;
     Wn5 = p_5 + A4*W;
     W_5=[W_5 Wn5];

 end
```

```
%Plotting All The W_i's and P_{ij}'s
x1=0:s:100;
x2=0:s:110;
x3=0:s:120;
x4=30:s:60;
x5=60:s:90;
figure(1)
plot3(W_1(1,:),W_1(2,:),x1,'b-o'); hold on
plot3(W_2(1,:),W_2(2,:),x2,'r-o'); hold on
plot3(W_3(1,:),W_3(2,:),x3,'k-o'); hold on
plot3(W_4(1,:),W_4(2,:),x4,'g-o'); hold on
plot3(W_5(1,:),W_5(2,:),x5,'m-o'); hold on
grid on
xlabel('W_x')
ylabel('W_y')
zlabel('Range of \phi_{ij}')
title('Locus of Moving Pivot W^i over Pole P_{12}')
plot(p_1(1,1),p_1(2,1),'k*'); hold on
text(p_1(1,1)-1,p_1(2,1)-1,4,'P_{12}','Color','black','FontSize',10)
plot(p_2(1,1),p_2(2,1),'k*'); hold on
text(p_2(1,1)+.5,p_2(2,1)+.5,4,'P_{13}','Color','black')
plot(p_3(1,1),p_3(2,1),'k*'); hold on
text(p_3(1,1)+.5,p_3(2,1)+.5,4,'P_{14}','Color','black')
plot(p_4(1,1),p_4(2,1),'k*'); hold on
text(p_4(1,1)-1,p_4(2,1)-1,4,'P_{23}','Color','black')
plot(p_5(1,1),p_5(2,1),'k*'); hold on
text(p_5(1,1)+.2,p_5(2,1)+.2,4,'P_{34}','Color','black')
plot(G(1,1),G(2,1),'k*'); hold on
text(G(1,1)+.2,G(2,1)+.2,4,'G','Color','black')
plot([p_1(1,1),p_4(1,1)],[p_1(2,1),p_4(2,1)],'k-')
```

```
plot([p_4(1,1),p_5(1,1)],[p_4(2,1),p_5(2,1)],'k-')
plot([p_5(1,1),p_3(1,1)],[p_5(2,1),p_3(2,1)],'k-')
plot([p_3(1,1),p_1(1,1)],[p_3(2,1),p_1(2,1)],'k-')
legend('Locus of Moving Pivots W^1 over P_{12}',
'Locus of Moving Pivots W^1 over P_{13}',
'Locus of Moving Pivots W^1 over P_{14}',
'Locus of Moving Pivots W^2 over P_{23}',
'Locus of Moving Pivots W^3 over P_{34}',
'Location of Poles')
```

# References


[1] Freudenstein, F. et al., "An analytical approach to the design of four-link mechanisms," *Transactions of the ASME*, Vol. 76, No. 3, 1954, pp. 442–483.

[2] Hall, A. S., *Kinematics and Linkage Design*, Waveland PressInc, 1986.

[3] Suh, C. H. and Radcliffe, C. W., *Kinematics and mechanisms design*, Wiley, 1978.

[4] Sandor, G. N. and Erdman, A. G., *Advanced Mechanism Design V. 2: Analysis and Synthesis*, Prentice-Hall, 1984.

[5] Roth, B., "Finite-Position Theory Applied to Mechanism Synthesis," *Journal of Applied Mechanics*, Vol. 34, 1967, pp. 599.

[6] Burmester, L. E. H., *Lehrbuch der kinematik: Für studirende der machinentechnik, mathematik und physik geometrisch dargestellt*, Vol. 1, A. Felix, 1888.

[7] Schoenflies, A., *Geometrie der Bewegung in synthetischer Darstellung*, BG Teubner, 1886.

[8] Beyer, R., "The Kinematic Synthesis of Mechanisms (Translated from German by H. Kuenzel),(1963)," .

[9] Hartenberg, R. and Danavit, J., *Kinematic synthesis of linkages*, New York: McGraw-Hill, 1964.

[10] Kimbrell, J. T., *Kinematics analysis and synthesis*, McGraw-Hill College, 1991.

[11] Luck, K. and Modler, K., "Konstruktionslehre der Getrebe," 1990.

[12] Paul, B., *Kinematics and dynamics of planar machinery*, Prentice Hall, 1979.

[13] McCarthy, J. M. and Soh, G. S., *Geometric design of linkages*, Vol. 11, Springer Science & Business Media, 2010.

[14] Freudenstein, F. and Sandor, G. N., "On the Burmester Points of a Plane," *Journal of Applied Mechanics*, Vol. 28, 1961, pp. 41.

[15] Waldron, K. J., Kinzel, G. L., and Agrawal, S. K., *Kinematics, dynamics, and design of machinery*, John Wiley & Sons, 2016.

[16] INNOCENTI, C., "Polynomial solution of the spatial Burmester problem," *Journal of mechanical design (1990)*, Vol. 117, No. 1, 1995, pp. 64–68.

[17] Li, D., Zhang, Z., and McCarthy, J. M., "A constraint graph representation of metamorphic linkages," *Mechanism and Machine Theory*, Vol. 46, No. 2, 2011, pp. 228–238.

[18] Kaufman, R., "Mechanism design by computer," *Machine Design*, Vol. 50, No. HS-025 808U, 1978.

[19] Waldron, K. and Song, S., "Theoretical and numerical improvements to an interactive linkage design program, RECSYN," *Proceedings of the Seventh Applied Mechanisms Conference*, 1981, pp. 8–1.

[20] Erdman, A. G. and Gustafson, J., "Lincages: Linkage interactive computer analysis and graphically enhanced synthesis package," *American Society of Mechanical Engineers (Paper)*, , No. 77-DET-5, 1977.

[21] Ruth, D. and McCarthy, J., "Sphinxpc: An implementation of four position synthesis for planar and spherical 4r linkages," *CD-ROM Proc. of the ASME DETC'97*, 1997, pp. 14–17.

[22] Ravani, B. and Roth, B., "Motion synthesis using kinematic mappings," *Journal of Mechanisms, Transmissions, and Automation in Design*, Vol. 105, 1983, pp. 460–467.

[23] Fox, R. and Willmert, K., "Optimum design of curve-generating linkages with inequality constraints," *Journal of Engineering for Industry*, Vol. 89, No. 1, 1967, pp. 144–151.

[24] Zimmerman, R. A., "Planar linkage synthesis for rigid body guidance using poles and rotation angles," *ASME 2013 International Design Engineering Technical Conferences and Computers and Information in Engineering Conference*, American Society of Mechanical Engineers Digital Collection, 2013.

[25] Bottema, O. and Roth, B., *Theoretical kinematics*, Vol. 24, Courier Corporation, 1990.

[26] MCCARTHY, J., "The synthesis of planar RR and spatial CC chains and the equation of a triangle," *Journal of mechanical design*, Vol. 117, No. B, 1995, pp. 101–106.

[27] Loerch, R., Erdman, A. G., and Sandor, G. N., "On the Existence of Circle-Point and Center-Point Circles for Three-Precision-Point-Dyad Synthesis," *Journal of Mechanical Design*, Vol. 101, No. 4, 1979, pp. 554–562.

[28] Loerch, R., Erdman, A. G., Sandor, G. N., and Midha, A., "Synthesis of Four Bar Linkages with Specified Ground Pivots," 1976.

[29] Martin, P. J., Russell, K., Lee, W.-T., and SODH, R. S., "An algorithm for planar four-bar motion generation with optimization," *Transactions of the Canadian Society for Mechanical Engineering*, Vol. 31, No. 3, 2007, pp. 357–371.

[30] Norton, R. L. et al., *Design of machinery: an introduction to the synthesis and analysis of mechanisms and machines*, Boston: McGraw-Hill Higher Education,, 2004.

[31] TING, K.-L., "Mobility criteria of single-loop N-bar linkages," *Journal of mechanisms, transmissions, and automation in design*, Vol. 111, No. 4, 1989, pp. 504–507.

[32] Chedmail, P. and Ramstein, E., "Robot mechanism synthesis and genetic algorithms," *Proceedings of IEEE international conference on robotics and automation*, Vol. 4, IEEE, 1996, pp. 3466–3471.